Nathalie J. Bureau, MD, received her medical degree and completed a diagnostic radiology residency at the University of Montreal. She completed a 1-year fellowship in musculoskeletal radiology at the University of Virginia Health Sciences Center. She is presently a staff radiologist in the Department of Radiology at Hôtel-Dieu de Montreal Hospital, Montreal, Quebec, Canada, where she is chief of the Musculoskeletal Section.

Robert G. Dussault, MD, received his BA degree at the Jean de Brébeuf College, Montreal, Quebec. He received his medical degree at the University of Sherbrooke, Sherbrooke, Quebec. He is presently professor of radiology and orthopedics at the University of Virginia Health Sciences Center and vice chair of the Department of Radiology.

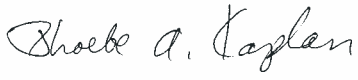

Phoebe A. Kaplan, MD, received her BS degree from the Nebraska Wesleyan University. She received her medical degree from the University of Nebraska College of Medicine. Her residency was completed at the University of Nebraska Medical Center. She is presently professor of radiology and orthopedics at the University of Virginia Health Sciences Center, where she is director of the Section of Musculoskeletal Imaging.

MRI OF THE KNEE: A SIMPLIFIED APPROACH

INTRODUCTION

The complementary role of magnetic resonance imaging (MRI) to more traditional musculoskeletal imaging modalities, such as plain films, arthrography, and computed tomography, makes it extremely valuable, and knee MRI has become the most commonly performed musculoskeletal MRI examination. Advantages of MRI are numerous: it is noninvasive; there is an absence of ionizing radiation; there are multiplanar imaging capabilities; and it offers superb and unsurpassed tissue contrast. In particular, MRI depicts soft-tissue structures like no other imaging modality before. The high accuracy of MRI in diagnosing pathologic conditions has supplanted arthroscopy as a diagnostic technique and transformed it into a therapeutic procedure.

Many radiologists have mastered the interpretation of knee MRI, and many papers have been written describing the best technique, various imaging sequences, and different signs and pitfalls in the interpretation of the images. So why write another review article on the subject?

This monograph is intended to be a step-by-step simplified approach to knee MRI. The first part, How to Set Up a Knee MRI Study, discusses in detail the necessary elements for realizing a good and easy-to-read knee MRI study. Step by step, the simple positioning of the patient in the magnet, the knee coils, the imaging sequences and parameters, and a set protocol are reviewed, explaining how an MRI study can be tailored to obtain the best results.

The next section is dedicated to normal anatomy of the knee, with emphasis on MRI appearance. Thus the osseous structures, cartilage, menisci, collateral and cruciate ligaments, quadriceps and patellar tendons, and joint capsule, as well as other smaller structures, are discussed and illustrated.

A Systematic Approach to Interpretation of Knee MRI is presented in the third section. Again, in a step-by-step fashion, a method of analyzing the many different images of a knee MRI study is proposed.

Finally, a complete review of the pathology of internal derangements of the knee is presented, including such entities as meniscal, ligamentous, and tendon tears, bone contusions and fractures, and degenerative joint disease. Pitfalls in interpretation that may deceive the inexperienced reader are reviewed. In addition, a section is devoted to cystic masses in and around the knee. Then the subject of arthritic disorders and anomalies of the bone marrow is also discussed. The different entities are illustrated with emphasis on the pertinent findings.

We hope this is a profitable review document for radiologists and a valuable teaching tool for residents.

HOW TO SET UP A KNEE MRI STUDY

The first step of any MRI study is to screen the patient for any potential ferromagnetic device, implant, or foreign body. Although uncommon, MRI-related injuries do occur, and screening patients before MRI imaging is mandatory and should be done by using a standardized protocol.[1,2]

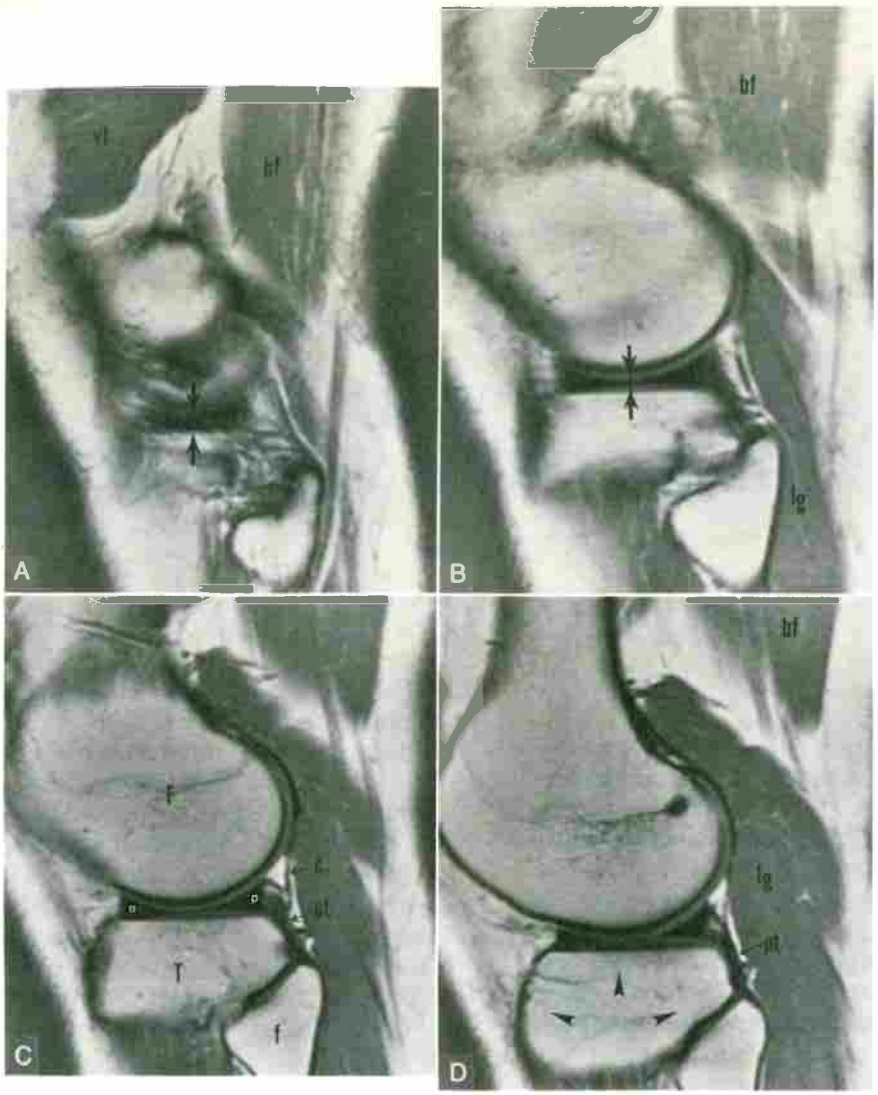

FIG 1. Normal knee. Four consecutive T1-weighted (TR/TE, 800/20) sagittal images through the lateral compartment of the knee joint. The two most lateral sections **(A, B)** show low-signal-intensity lateral meniscus (arrows) with the bow-tie configuration where the anterior and posterior horns are connected by the body of the meniscus. Note the rapid tapering of the body of the meniscus. **C,** An adjacent section toward the intercondylar notch shows the anterior (a) and posterior (p) horns of the lateral meniscus of nearly equal size. **D,** The next section toward the intercondylar notch demonstrates the flat articular surface of the lateral tibial plateau and the tuberosity projecting posteriorly and articulating with the fibular head (arrowheads). F, femur; T, tibia; f, fibula; c, joint capsule; bf, biceps femoris; vl, vastus lateralis; lg, lateral head of gastrocnemius muscle; pt, popliteus tendon.

POSITIONING

Once the study has been authorized, the patient is positioned supine with the extremity in slight external rotation of approximately 15 degrees. In this position, the anterior cruciate ligament (ACL), which runs obliquely in the sagittal plane, is best visualized.[3] Most patients when lying supine have a natural tendency to rotate the extremity externally, and so the technologist has to provide padding only around the knee, mainly to ensure the most comfortable position so the patient will be able to remain immobile during the entire examination. Immobility will eliminate any potential motion artifact that would degrade the image quality. Certain authors also advocate positioning the knee with 5 degrees of flexion to permit optimal evaluation of patellar alignment on cross-sectional images, because hyperextension of the knee may cause overestimation of patellar subluxation.[4] This positioning of the knee with 5 degrees of flexion should be carefully monitored by the technologist because too much flexion may impair the correct visualization of the ACL.[5]

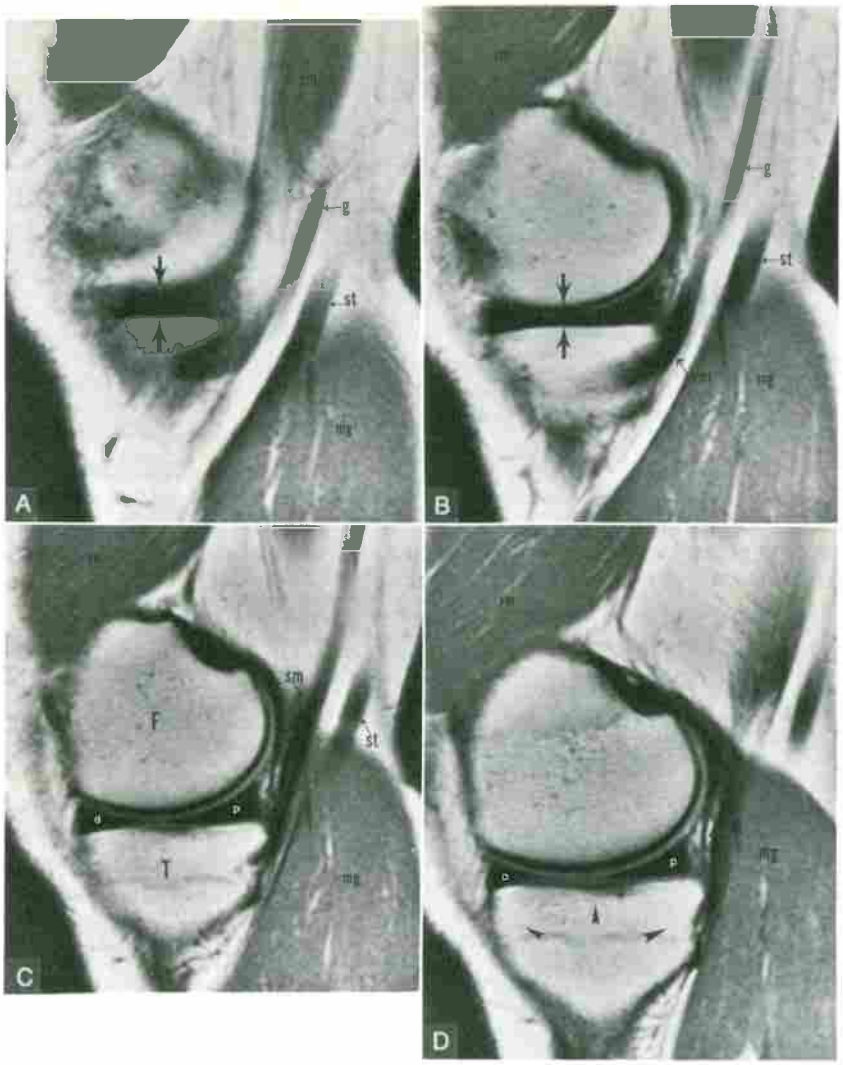

FIG 2. Normal knee. Four consecutive T1-weighted (TR/TE, 800/20) sagittal images through the medial compartment of the knee joint. The two most peripheral sections **(A, B)** show the normal bow-tie appearance of the medial meniscus (arrows). Two consecutive adjacent sections toward the intercondylar notch **(C, D)** demonstrate the normal configuration of the anterior (a) and posterior (p) horns of the medial meniscus. The posterior horn is approximately twice as large as its anterior counterpart. Note the symmetric shape of the medial tibial plateau and its slightly concave articular surface (arrowheads). F, femur; T, tibia; c, joint capsule; vm, vastus medialis; sm, semimembranosus muscle; g, gracilis tendon; st, semitendinosus tendon; mg, medial head of gastrocnemius muscle.

KNEE COILS

MRI can be performed using either body or surface coils. To obtain optimal images of the knee, use of a dedicated surface coil is mandatory. Surface coils improve signal-to-noise ratios, which results in better spatial resolution and allows precise depiction of normal anatomy and detection of sometimes subtle abnormal findings.[6] Two major types of surface coils are available: receive-only and transmit-and-receive coils. The latter are preferred because they eliminate ghost image artifact from the opposite knee, thus further improving the image quality. In addition, one has a choice between flexible wraparound or rigid cylindrical or quadrature-type surface coils; both types of coils give excellent images.

IMAGING SEQUENCES

Musculoskeletal MRI is performed mainly with spin-echo sequences. Spin-echo sequences use a 90-degree excitation radiofrequency (RF) pulse followed by a 180-degree refocusing pulse. The echo produced is then mathematically processed by the computer and transformed into the final image.

T1-weighted (T1W) sequences are particularly

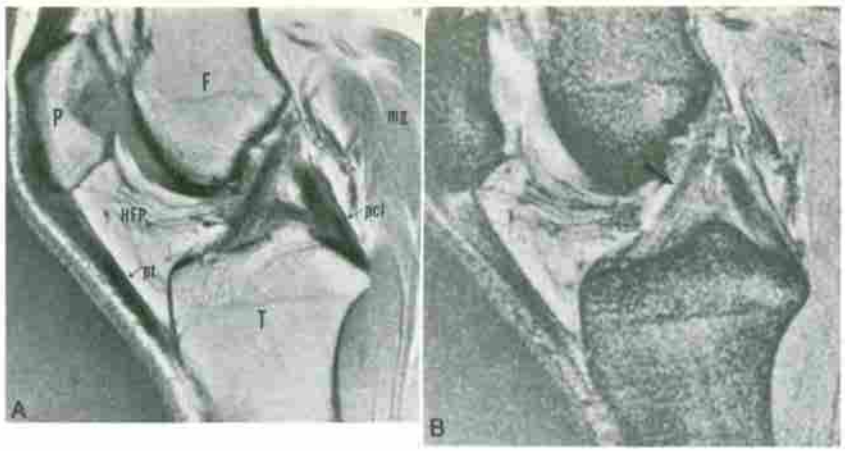

FIG 3. Normal anterior cruciate ligament (ACL). Sagittal T1-weighted (TR/TE, 600/14) **(A)** and gradient-echo (TR/TE, 500/20; angle, 30 degrees) **(B)** images through the intercondylar notch demonstrate the normal ACL as a low-signal-intensity structure extending from the lateral femoral condyle to its distal tibial insertion at an angle almost parallel to the roof of the intercondylar notch (arrow). Note the normal striated appearance of the distal segment of the ACL, best demonstrated on the gradient-echo image. F, femur; T, tibia; P, patella; pt, patellar tendon; pcl, PCL; mg, medial head of gastrocnemius muscle; HFP, Hoffa fat pad.

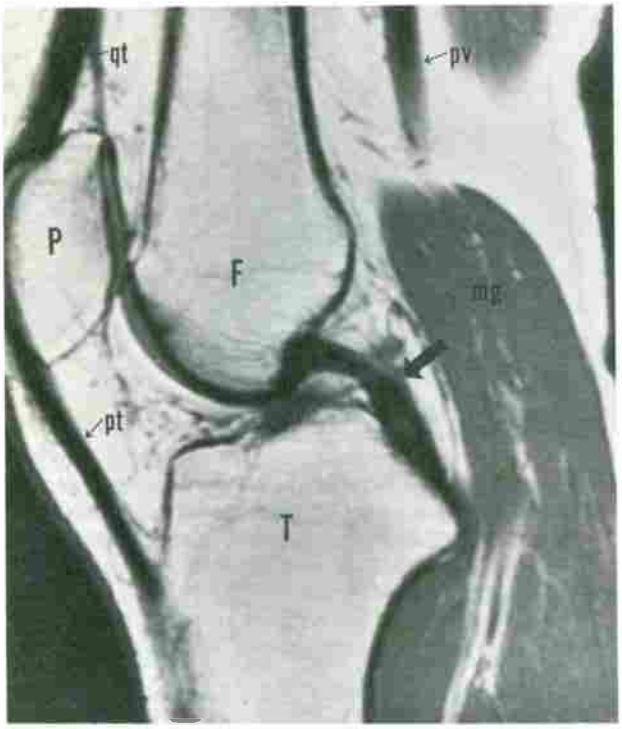

FIG 4. Normal posterior cruciate ligament (PCL). Sagittal T1-weighted (TR/TE, 800/20) image through the intercondylar notch shows the normal course and configuration of the PCL, which extends from the posterior aspect of the intercondylar eminence, well below the joint line, to the medial femoral condyle (arrow). The normal PCL has diffuse low-signal intensity on all pulse sequences. Note the normal homogeneous high signal intensity of fatty marrow of the different osseous structures. F, femur; T, tibia; P, patella; pt, patellar tendon; qt, quadriceps tendon; mg, medial head of gastrocnemius muscle; pv, popliteal vessel.

suited to evaluate anatomy and bone marrow. T1W sequences use a short repetition time (TR) and short echo time (TE). The usual range of TR for T1W sequences is 400 to 700 msec, and for TE, usually 17 to 25 msec.

The TR is related to the area imaged. The longer the TR, the larger the anatomic coverage allowed. A TR of 800 may be required to cover the entire knee in one sequence. A TR of 400 will take far less time but not cover the entire knee. Using a short TR, two sets of sequences will be required to cover the knee; this has the advantage of leaving no gaps between slices, eliminates cross-talk, and if a patient moves, only half the time is required to repeat the short TR sequence.

The TE is related to the RF pulse. The longer the TE, the longer the RF pulse and the more time allowed to refine the slice profile. This means that image resolution is less affected by cross-talk, and minimal slice distance may be used, which decreases loss of anatomic coverage in interslice gaps. On the other hand, with a short TE, a short RF pulse is selected, and more cross-talk will appear between slices, degrading the image resolution. Thus sequences using a short TE require use of some slice distance (>10%) or use of interleaved slices (100% gap). Interleaved technique necessitates acquiring two separate sets of slices, which means two sequences must be done to cover the anatomic area in one plane. Thus the entire area can be covered without a penalty for using a short TE.

T2W sequences use a long TR and a long TE. In musculoskeletal MRI, a TR between 2000 and 2500 msec and a TE between 80 and 100 msec are generally used. With such high TR values, a large

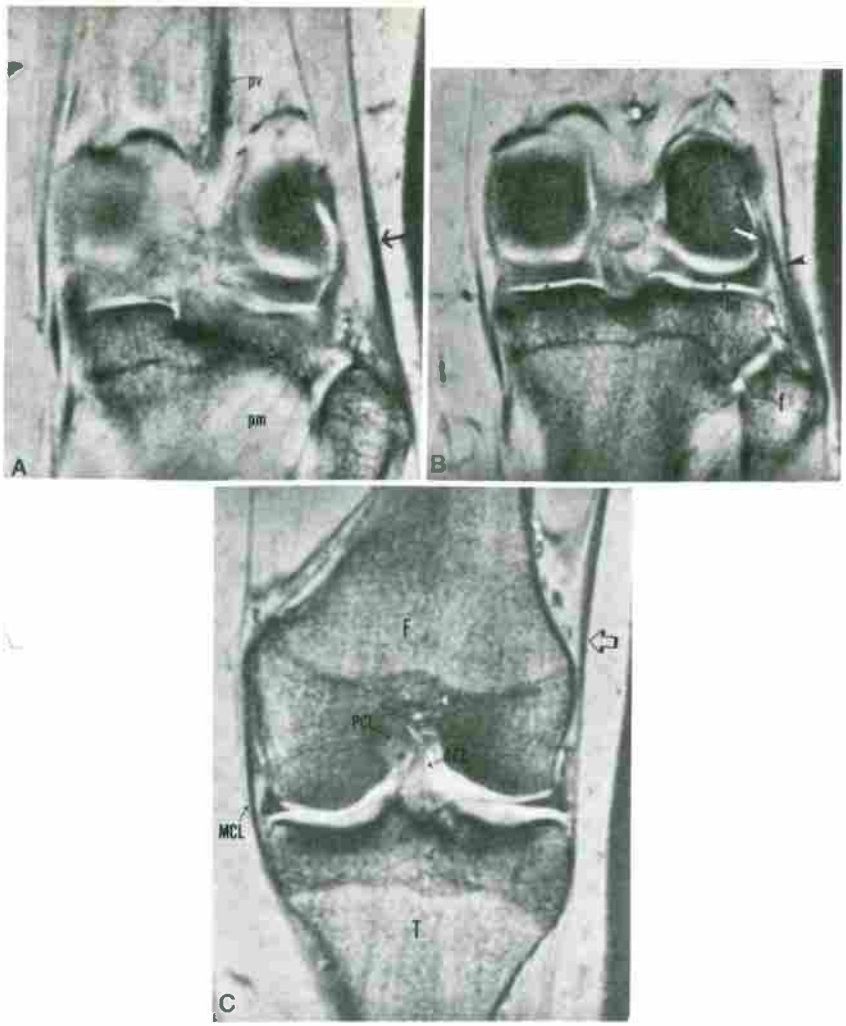

FIG 5. Normal coronal anatomy. Gradient echo (TR/TE, 500/20; angle, 30 degrees). The most posterior section **(A)** depicts the biceps femoris tendon (arrow) as a low-signal-intensity band-like structure inserting on the fibular head. Immediately adjacent anterior section **(B)** demonstrates the lateral collateral ligament (LCL) (arrowhead) with its oblique course, extending between the lateral femoral epicondyle and fibular head. Note the superior extension of the popliteus tendon (white arrow) between the lateral femoral condyle and LCL. **C,** A third section at the level of the intercondylar eminence tubercles, shows the iliotibial band (open arrow). F, femur; T, tibia; f, fibula; mm, medial meniscus; lm, lateral meniscus; MCL, medial collateral ligament; pm, popliteus muscle; pv, popliteal vessel; ACL, anterior cruciate ligament; PCL, posterior cruciate ligament.

area can be covered. T2W sequences are good to image marrow, fluid, and some soft-tissue lesions but are less valuable for imaging fibrous and ligamentous structures than are certain other sequences. In addition, with a long TR, the imaging time is long, which increases the risk of motion artifact.

A long TR and a short TE yield proton density–weighted images. Proton density is also referred to as the first echo of a double-echo T2W spin-echo sequence. TR will be in the same range as for a T2W sequence, between 2000 and 2500 msec, but the TE is shorter, usually between 20 and 40 msec. Proton density offers very little advantage in musculoskeletal imaging, mainly because the conspicuity of lesions is poor because of little difference in signal between normal marrow and abnormalities.

Pulse sequences other than spin echo have been developed in an effort to decrease imaging time and to optimize conspicuity of certain pathologic conditions. Gradient-echo imaging is used in place of T2W spin-echo sequences for musculoskeletal MRI by many radiologists. As opposed to spin-echo sequences, gradient-echo imaging uses a smaller (<90 degree) excitation RF pulse and a gradient refocusing, rather than a 180-degree RF refocusing, pulse to produce an echo. Gradient-echo sequences can be relatively T1W images (spoiled gradient-echo sequences) or relatively T2W images (steady-state gradient-echo sequences or T2 star

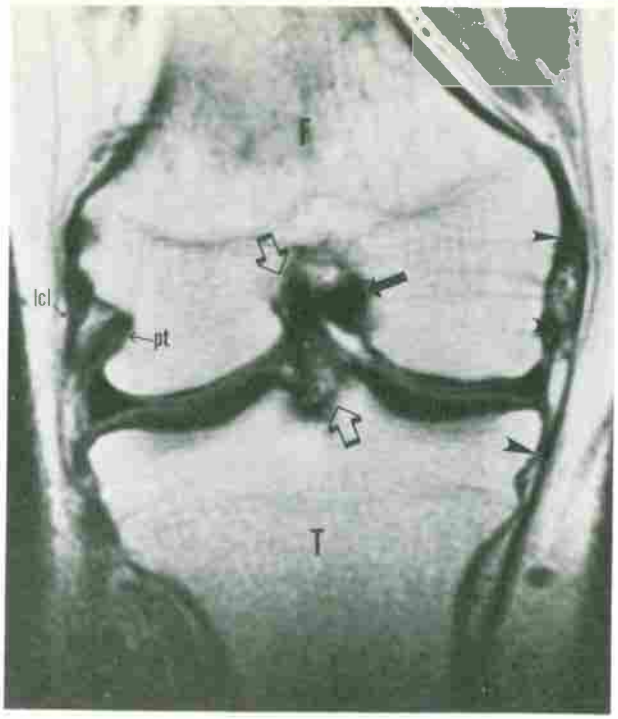

FIG 6. Normal knee. T1-weighted (TR/TE, 800/20) coronal image at the level of the intercondylar eminence tubercles shows the normal MCL as a thin low-signal-intensity band (arrowheads) coursing from the medial femoral epicondyle to the proximal tibial diametaphysis. The normal posterior cruciate ligament appears in cross-section in the medial side of the intercondylar notch (arrow). In the distal segment, the normal ACL has an oblique course in the lateral aspect of the intercondylar notch (open arrows). F, femur; T, tibia; lcl, lateral collateral ligament; pt, popliteus tendon.

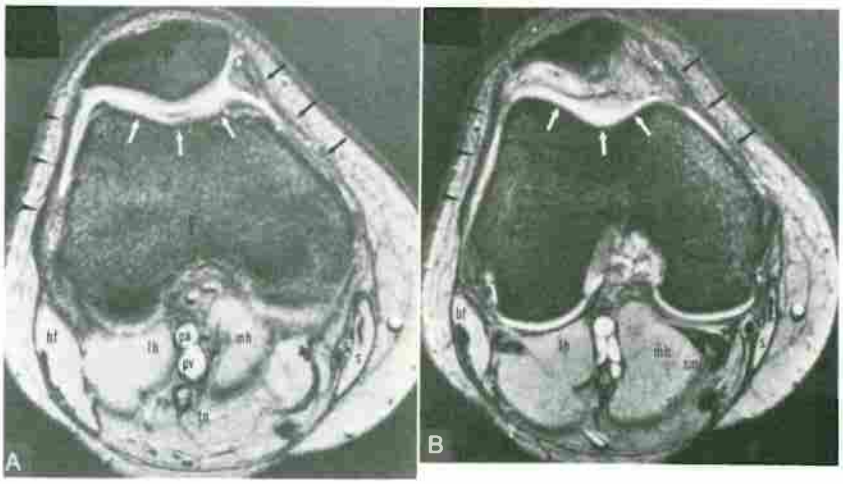

FIG 7. Normal knee. Gradient echo (TR/TE, 578/18; angle, 30 degrees) axial images at the level of the midsection **(A)** and inferior pole **(B)** of the patella, respectively. Normal appearance of the patellofemoral joint with the patella resting symmetrically in the trochlear groove (white arrows). The medial (black arrows) and lateral (arrowheads) retinacula are low-signal-intensity bands. F, femur; P, patella; bf, biceps femoris muscle; lh, lateral head of gastrocnemius muscle; mh, medial head of gastrocnemius muscle; sm, semimembranosus tendon; st, semitendinosus tendon; g, gracilis tendon; s, sartorius muscle; pa, popliteal artery; pv, popliteal vein; tn, tibial nerve.

[T2*] images). T2* sequences show joint fluid well, which acts as a natural contrast agent. Typical T2* parameters are 400/17, TR/TE, with a 30-degree flip angle. The flip angle refers to the excitation RF pulse that is applied to the protons. It will generate the transverse magnetization, which will produce the signal used to create the image.

Contrast in gradient-echo imaging depends largely on the flip angle used. Using a short TR and a smaller flip angle reduces significantly the imag-

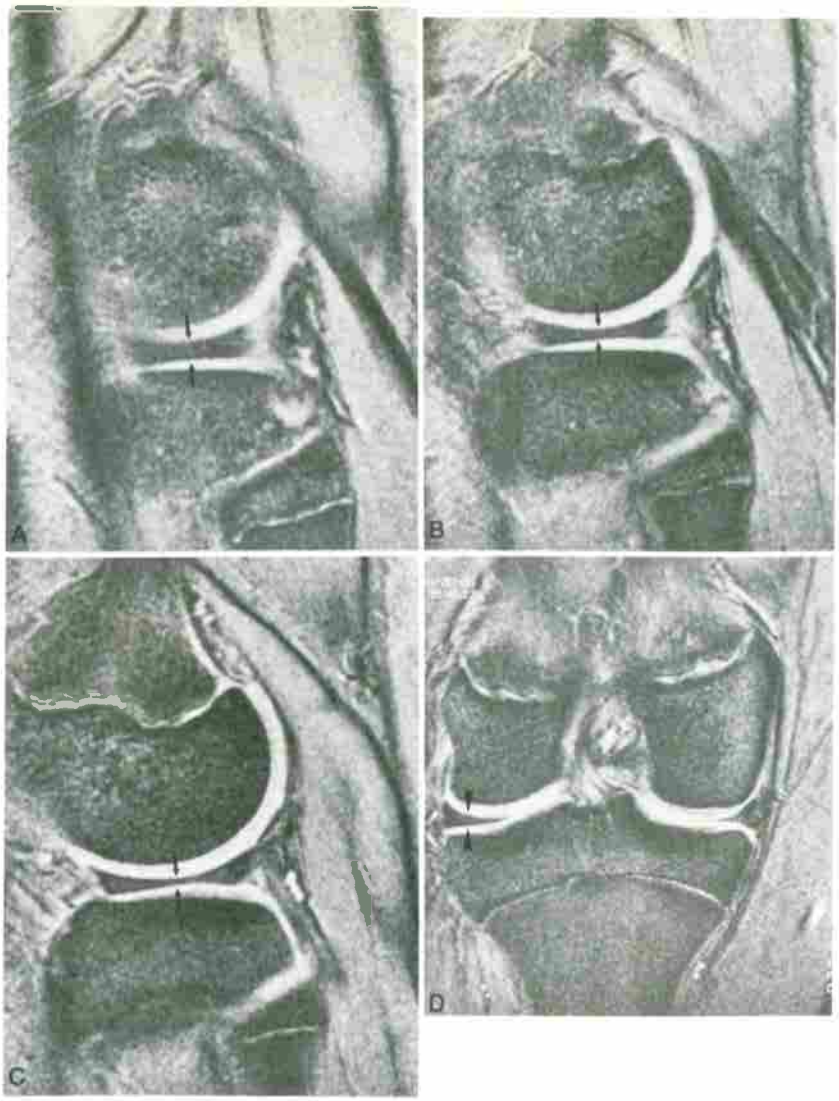

FIG 8. Discoid lateral meniscus. Sequential adjacent gradient echo (TR/TE, 578/18; angle, 30 degrees) (4 mm cuts) sagittal images **(A, B, C),** beginning at the periphery of the lateral meniscus, demonstrate the bow-tie configuration (arrows) on three images, indicating the body of the meniscus is abnormally large in the mediolateral dimension. **D,** Coronal image at the level of the intercondylar eminence tubercles shows a normal triangular configuration of the lateral meniscus, but it is abnormally thick in height (arrowheads), as compared to the medial meniscus.

ing time, and T2* images can normally be performed in about half the time it takes to obtain T2W sequences. T2* is excellent to image cartilage, effusion or other fluid, soft-tissue lesions, and is particularly good for depicting fibrous and ligamentous structures. T2* increases contrast between adjacent tissues; therefore subtle contrast differences are easily seen, and tears of menisci and ligaments are more easily diagnosed than with spin-echo T2W images.[7] T2* sequences are not reliable for imaging marrow lesions, but these are shown well on T1W images, which are always obtained as part of a standard knee MRI examination.

Three-dimensional (3-D) volume acquisition gradient-echo MRI offers certain advantages over regular 2-D gradient-echo imaging. With 3-D gradient-echo imaging, one can obtain very thin (1 mm or less) contiguous sections, which increases significantly the spatial resolution, without losing information because of intersection gaps. In addition, no cross-talk occurs, reducing volume averaging to a minimum. Because of the small slice thickness, the signal-to-noise ratio is lower than with thicker 2-D imaging. Acquisition of data is performed in one plane, with subsequent reconstruction of images in any other plane. Images are best in the plane that data are acquired in and decrease in quality the further one moves from the plane of

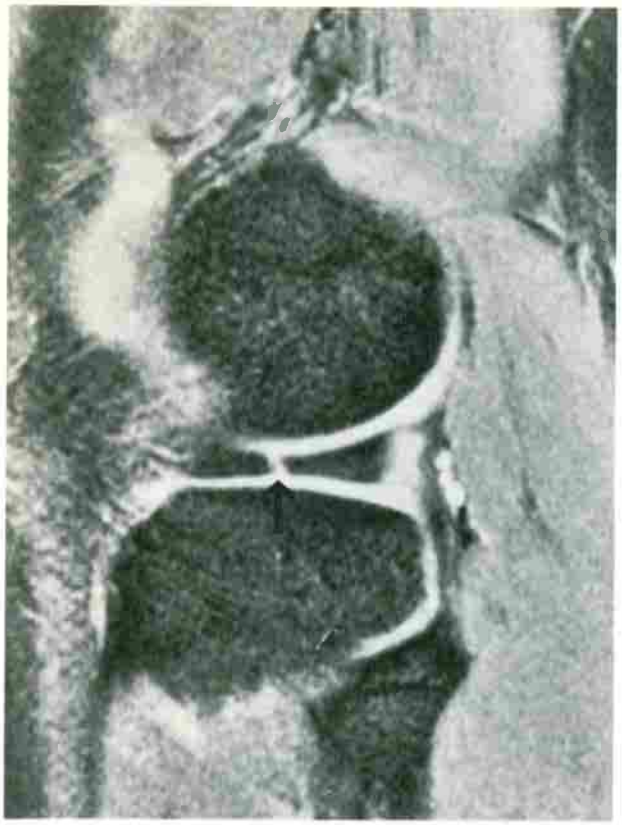

FIG 9. Radial tear of lateral meniscus. Sagittal gradient echo (TR/TE, 400/18; angle, 30 degrees) image through peripheral portion of lateral meniscus shows a vertical high-signal-intensity line (arrow) extending to the articulating surfaces, indicating a radial tear through the body of the lateral meniscus.

imaging. This technique has been shown to be accurate in diagnosing meniscal and ligamentous tears, as well as thinning of hyaline cartilage.[8,9] This 3-D volume gradient echo may be useful in certain circumstances in which exceptionally thin cuts are required to make a diagnosis that is not possible with standard section, such as a difficult-to-identify ACL.

Fat-suppression techniques can be valuable in the evaluation of bone marrow disorders.[7,10-12] Two of the most frequently used methods are fat-saturation, which can be used with spin-echo T1W or T2W sequences, as well as with gradient-echo sequences and short-T1 inversion recovery (STIR) images. Suppression of the relatively high signal intensity of fat increases the contrast between normal marrow and high-signal-intensity lesions. Processes such as bone contusions, marrow edema, osteonecrosis, osteomyelitis, as well as primary or metastatic tumor, are more conspicuous than they are without the use of fat-suppression techniques. Fat-suppression techniques in conjunction with spin-echo T1W images provide an excellent means of demonstrating the extent as well as presence of bone marrow involvement by disease. In the routine MRI evaluation for internal derangement of the knee, fat-suppression techniques increase detection of bone contusions and, by increasing conspicuity of soft-tissue edema, may also aid in the diagnosis of ligamentous injury.[7]

IMAGING PARAMETERS

Setting up a knee MRI study requires, in addition to deciding which pulse sequences to use, determining the different imaging parameters that will affect signal intensity, spatial resolution, and geometrical coverage. These parameters may be modified to optimize image quality.

The signal intensity, also referred to as signal-to-noise ratio, is mainly influenced by the external magnetic field strength and the voxel size. The voxel size will also affect the image resolution.

High magnetic field strengths are desirable because they provide a stronger MR signal to be received. A voxel is defined as the volume element in the body corresponding to one picture element or pixel in the image. The voxel size corresponds to a concentration of protons that contribute to produce the signal. The dimensions of the voxel are defined by the slice thickness and the field of view (FOV) divided by the matrix size. Although the external magnetic field strength is predetermined by the type of MR machine (0.5T, 1.0T, 1.5T) used, the slice thickness, FOV, and matrix size are operator-controlled parameters to be set for each MRI study.

The influence of the slice thickness on image quality is twofold. Resolution of anatomic detail is increased with use of thin slices but, at the same time, the voxel size is smaller, which yields lower signal intensity. The converse is also true.

Manipulating the FOV will affect image resolution and signal intensity in a similar fashion. The maximum FOV that can be used is predetermined for each type of coil. For imaging the small anatomic structures of joints, a small FOV is preferred.

The matrix is determined by phase and frequency encoding. These two different processes are used for encoding the image information into the excited slice. The effect of changing matrix size on image resolution and signal intensity is somewhat complex. As a general rule, the larger the matrix size (assuming FOV and slice thickness remain constant), the higher the spatial resolution and the lower the signal intensity.

The signal received can be measured repeatedly and averaged. This is referred to as the number of acquisitions or number of excitations. The signal-to-noise ratio is improved with the square root of

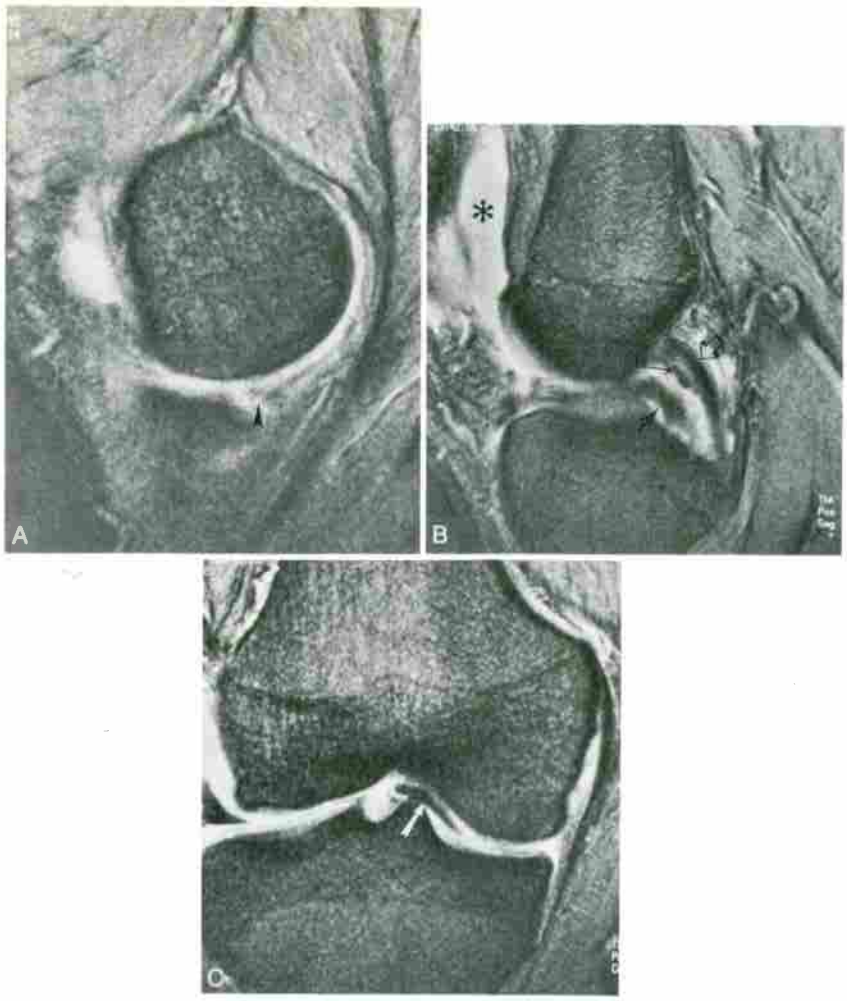

FIG 10. Bucket-handle tear with displaced fragment. **A,** Sagittal gradient echo (TR/TE, 442/18; angle, 30 degrees) image through the periphery of medial meniscus shows absence of the normal bow-tie configuration and a small irregular remnant of the posterior meniscal horn (arrowhead). **B,** Sagittal gradient echo (same parameters) image through the intercondylar notch demonstrates "double posterior cruciate" sign formed by the displaced inner meniscal fragment (arrow) lying inferior and parallel to the PCL (open arrow). **C,** Coronal gradient echo (TR/TE, 578/18; angle, 30 degrees) shows the inner meniscal fragment (white arrow) displaced into the intercondylar notch. Note the absence of meniscal substance peripherally. *, joint effusion in suprapatellar pouch; lh, ligament of Humphry.

the number of acquisitions. The image resolution is not affected. Using multiple acquisitions may improve signal intensity but at the expense of increasing imaging time. This introduces the concept of total acquisition time. Three factors determine the time to image: time to repetition (TR), number of acquisitions and number of views acquired per image, and number of phase-encoding steps. This should be taken into consideration when setting up a pulse sequence.

The geometric coverage, also referred to as anatomical coverage, is mainly determined by the number of slices and slice orientation (axial, coronal, sagittal). Contrast is mainly influenced by the sequence used (spin echo T1W, T2W, gradient echo).

Another important factor in MR imaging is the occurrence of artifacts. In knee MRI, two artifacts are to be considered: the motion artifact, which will always occur in the phase direction of the image, and the chemical-shift artifact, which will arise in the frequency (or read) direction of the image. It will become important for imaging the knee in different planes to reorient (swap) the phase-encoding gradient to prevent alteration of the image by motion artifact arising from the popliteal artery. When doing so in the sagittal plane, this will automatically reorient the frequency-encoding gradient in the anteroposterior direction, and the chemical shift artifact will then appear on the anterior and posterior aspects of the femur instead of appearing at the weight-bearing surface of the femorotibial joint, where it can impair analysis of the meniscus.

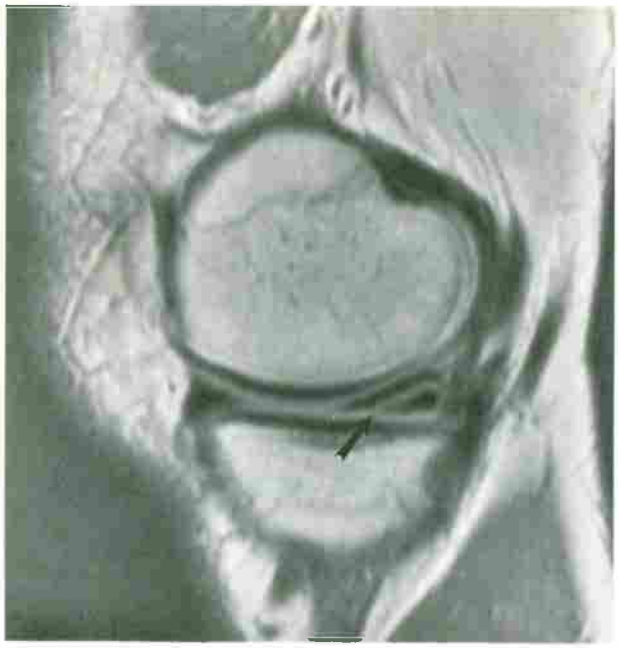

FIG 11. Horizontal meniscal tear. Sagittal T1-weighted (TR/TE, 800/20) image demonstrates high-signal-intensity line extending to the inferior articular surface of the posterior horn of the medial meniscus (arrow), representing a horizontal cleavage tear.

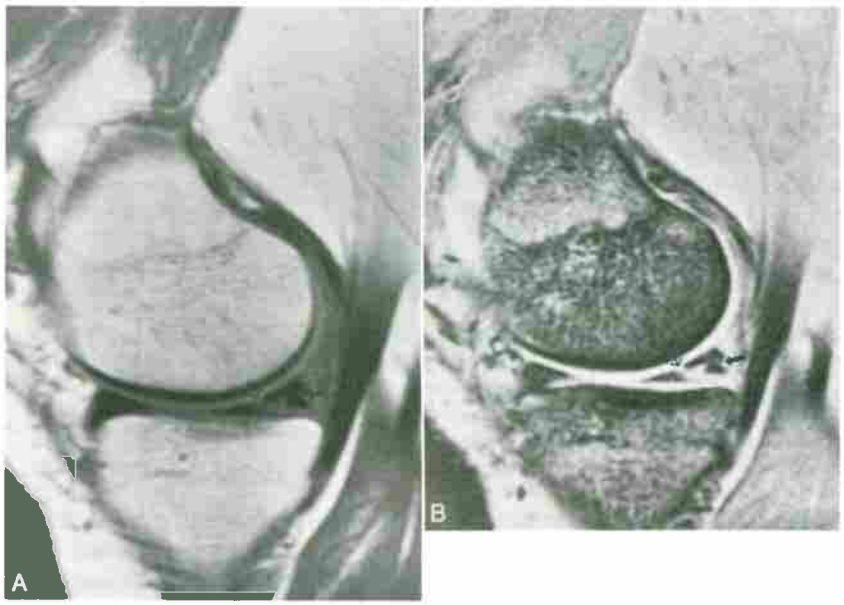

FIG 12. Complex meniscal tear. **A,** Sagittal T1-weighted (TR/TE, 800/20) and **B,** gradient echo (TR/TE, 450/20; angle, 30 degrees) images through the medial meniscus show high-signal-intensity linear tears with vertical (thin arrow) and horizontal (thick arrow) orientations though the posterior meniscus. Note the increased conspicuity of the tears on the gradient-echo image, **B.**

IMAGING PROTOCOL

Clearly, there are many possible choices of sequences and imaging parameters, and each has its own unique advantages and disadvantages. It is not practical, however, to monitor and tailor each knee MRI examination to the specific patient and problem. It is much more desirable to arrive at a standard MRI protocol that adequately evaluates (in a short period) the structures of the knee for the routine indications of pain or internal derangement. Several different protocols accomplish these goals equally well, but here we discuss the protocol we currently use with a Siemens 1.5T machine.

Our standard protocol for examination of the knee (Table 1) begins with an axial gradient-echo scan: TR/TE, 600/18 msec, flip angle 30 degrees, with 4 mm contiguous slices, with an interslice gap of 20%, FOV of 280 cm, a 384 × 512 matrix, and one acquisition. (With a General Electric ma-

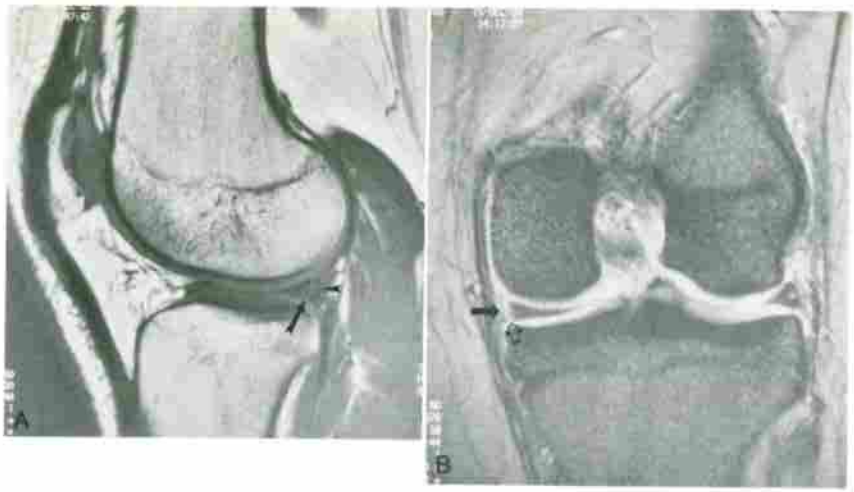

FIG 13. Meniscocapsular separation. **A,** T1-weighted (TR/TE, 430/20) sagittal image of medial meniscus shows a vertical high-signal-intensity tear (arrow) through the most peripheral aspect of the posterior meniscus. A fragmented small segment of the meniscus (arrowhead) is separated from the remainder of the posterior horn. **B,** Coronal gradient echo (TR/TE, 578/18; angle, 30 degrees) image again demonstrates the vertical tear (open arrow) and small detached fragment (solid arrow) with increased conspicuity, confirming the diagnosis.

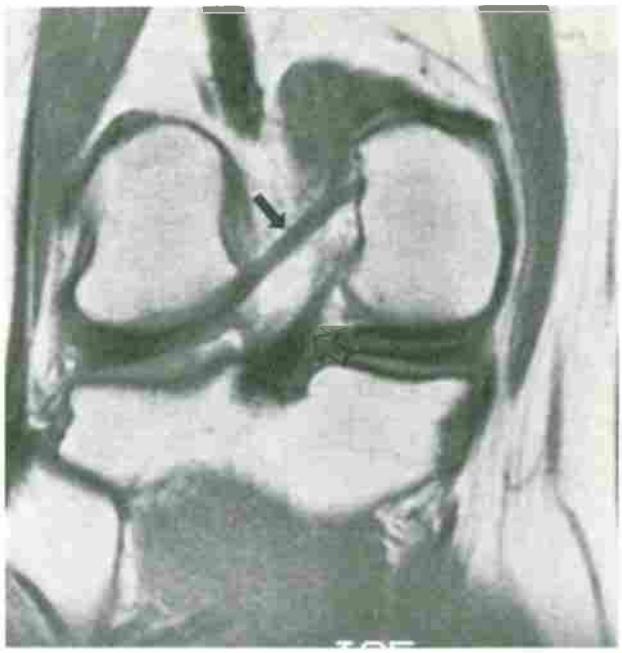

FIG 14. Meniscofemoral ligaments. Coronal T1-weighted (TR/TE, 800/20) image demonstrates the ligament of Wrisberg (solid arrow) extending from the posterior horn of the lateral meniscus to the medial femoral condyle. Note the proximal segment of the posterior cruciate ligament (open arrow) coursing vertically.

chine, using the "no phase wrap" option, the matrix size is actually half this). Based on this transverse sequence, T1W (TR/TE, 600/20 msec) and T2* (TR/TE, 600/18 msec, flip angle 30 degrees) sagittal images are obtained covering the entire knee from medial to lateral. Other parameters for the sagittal sequences are interleaved (100% interslice gap) 4 mm contiguous slices, FOV of 280 cm, a 384 × 512 matrix, and one acquisition. Then using the same parameters as for the T2* sagittals, coronal images are obtained, again based on the axial scan covering the knee from the patella to the posterior aspect of the knee. In this last sequence, anatomic coverage is obtained with 4 mm slices with a 20% interslice gap. Imaging in all three planes is performed with the frequency- and phase-encoding gradients being swapped.

NORMAL ANATOMY WITH MRI CORRELATION

OSSEOUS STRUCTURES

The knee is the largest joint in the body. It is a hinge joint and has the greatest range of motion in

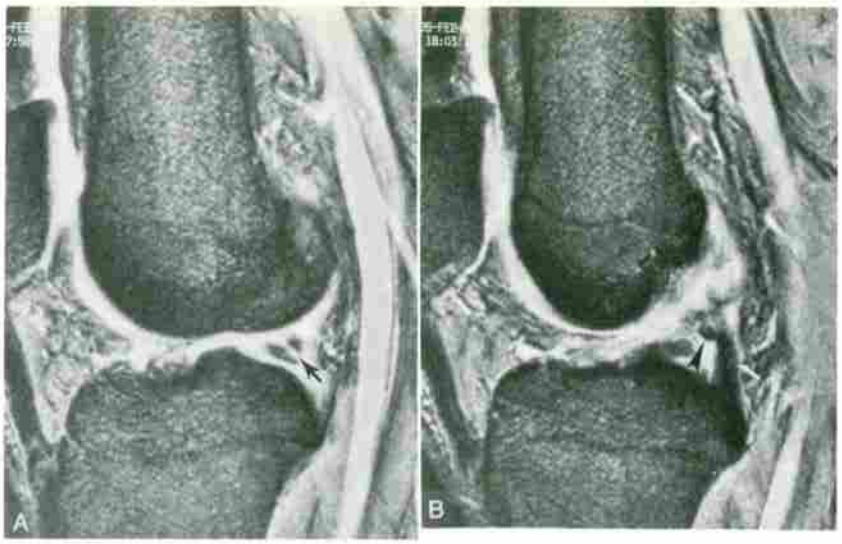

FIG 15. Pseudomeniscal tear. **A,** Sagittal gradient-echo (TR/TE, 442/18; angle, 30 degrees) image shows a pseudotear (arrow) of the posterior horn of the lateral meniscus (anteriorly) created by the proximity of the ligament of Humphry (posteriorly). **B,** Adjacent sagittal image demonstrates the ligament of Humphry (arrowhead) in cross-section anterior to the PCL (white arrow). Mass of edema/hemorrhage from acute anterior cruciate tear (open arrow).

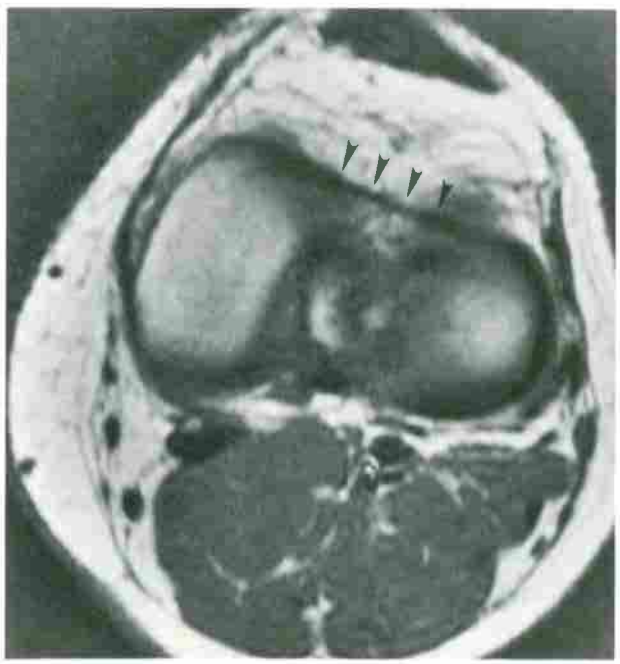

FIG 16. Transverse meniscal ligament. Axial T1-weighted (TR/TE, 600/20) image demonstrates the transverse meniscal ligament (arrowheads) extending between the anterior horns of the medial and lateral menisci.

flexion. Because it is located at the end of two long lever arms, the tibia and the femur, the knee is subjected to a significant amount of stress and is particularly susceptible to trauma.[13] Stability of the knee joint is provided mainly by the articular capsule reinforced by external ligaments, the collateral and cruciate ligaments, and surrounding muscles and tendons. The external ligaments reinforcing the capsule are the fascia lata and the iliotibial tract; the medial and lateral patellar retinacula; and the patellar, oblique popliteal, and arcuate popliteal ligaments.[14]

A standard knee MRI study will include the distal femur, proximal tibia and fibula, as well as the patella. Other osseous structures that can normally be seen are two sesamoid bones: the fabella in the lateral head of the gastrocnemius tendon and the cyamella, which is embedded in the popliteus tendon.[4]

The lower end of the femur, with its two prominent articular masses, provides a bearing surface for the transmission of the body weight to the proximal tibia. The femoral condyles are partially covered with hyaline cartilage, providing an articular surface with the patella above and tibial plateaus below. The articular surface of the femur that articulates with the patella is concave and extends higher on the lateral than on the medial side; thus, articulation with the patella occurs mainly with the lateral femoral condyle. Anteriorly, the articular surface of the two condyles is continuous, and posteriorly, it is interrupted by the intercondylar notch. The lateral condyle is not as prominent as the medial condyle but is stronger. It is more directly in line with the femoral shaft, so probably assumes more of the transmission of the weight to the tibia. Both condyles have a bony prominence on their respective medial and lateral sides corresponding to the medial and lateral epicondyles.[15]

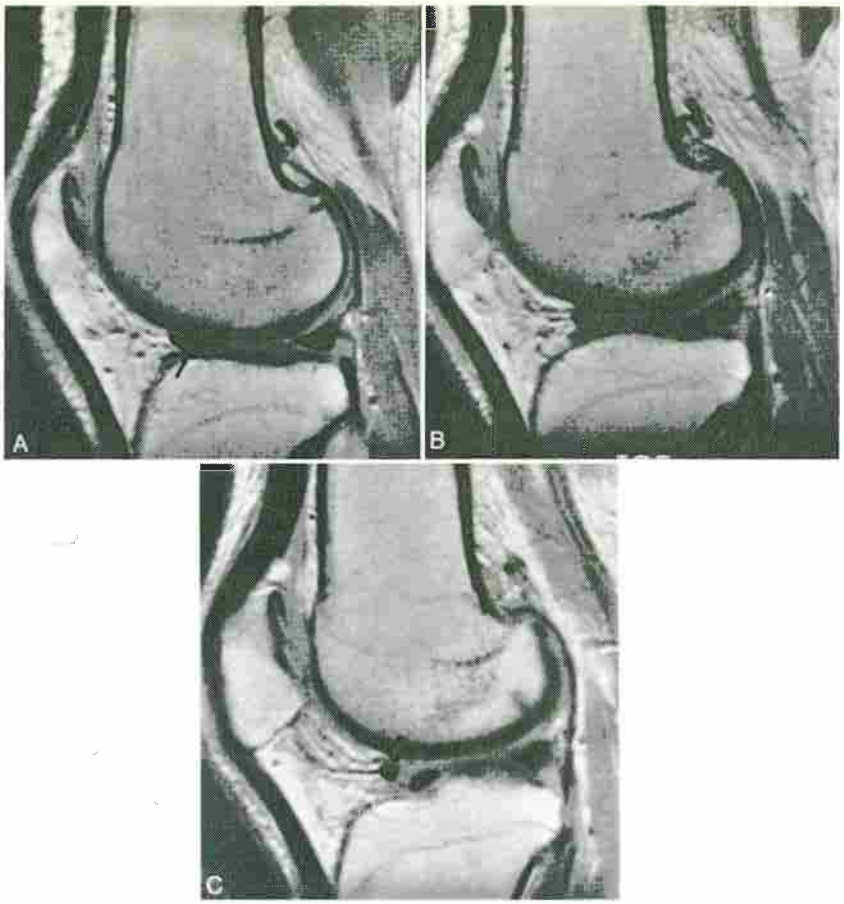

FIG 17. Pseudomeniscal tear. Consecutive sagittal T1-weighted (600/20) images. **A,** A fine high-signal-intensity line (thin arrow) between the closely apposed transverse meniscal ligament (anteriorly) and anterior horn of lateral meniscus (posteriorly) simulates a meniscal tear. **B, C,** Two adjacent images prove the continuity with the transverse meniscal ligament (thick arrow).

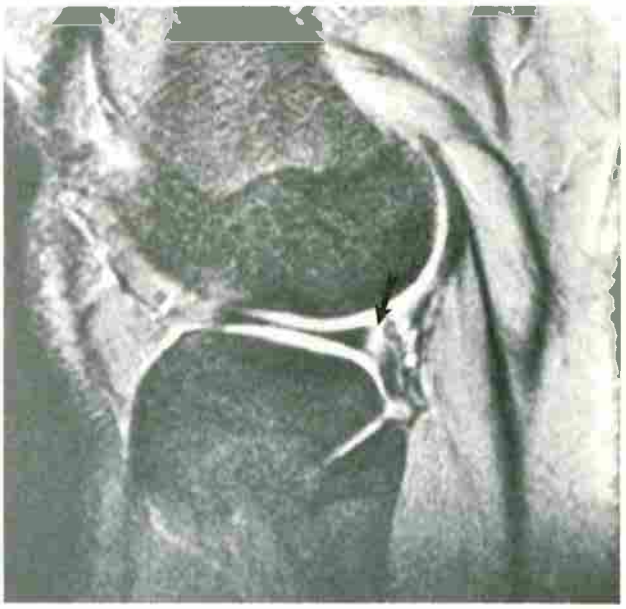

FIG 18. Pseudomeniscal tear. Sagittal gradient-echo (TR/TE, 460/18; angle, 30 degrees) image through the lateral meniscus shows a high-signal-intensity line (arrow) formed between the posterior horn of the lateral meniscus and popliteus tendon, which may simulate a peripheral tear or meniscocapsular separation.

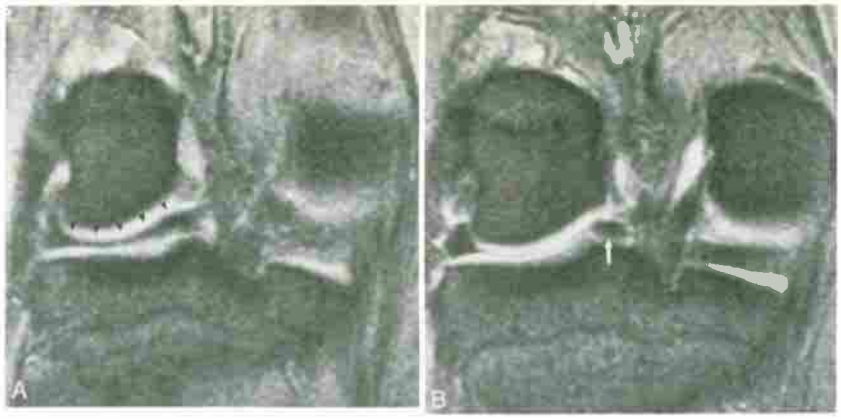

FIG 19. Pseudo–bucket-handle tear. Coronal gradient-echo (TR/TE, 50/20; angle, 30 degrees) images of posterior aspect of the knee. **A,** The most posterior section shows the posterior horn of the medial meniscus as a continuous low-signal-intensity structure (arrowheads). On the anterior adjacent section, **B,** a bucket-handle tear with a displaced inner fragment (white arrow) is simulated. This pitfall is caused by the "C" shape configuration of the meniscus.

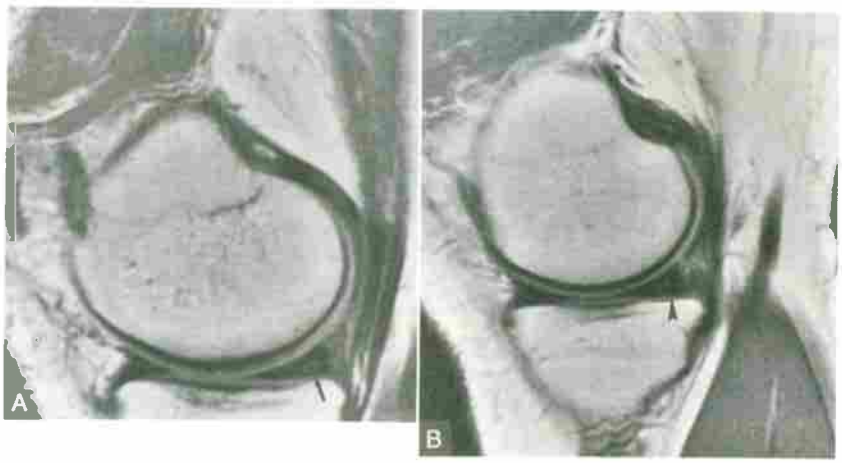

FIG 20. Meniscal degeneration. Sagittal T1-weighted (TR/TE, 800/20) images. **A,** Round area of intrameniscal high signal intensity (arrow) due to mucoid degeneration. **B,** A different patient with linear grade 2 signal (arrowhead) again not traversing the articular surface.

The proximal end of the tibia is formed by two prominent articular masses, the medial and lateral plateaus, and a smaller projection, the tuberosity of the tibia, which gives rise to the distal attachment of the patellar tendon. The medial tibial plateau is larger, oval in shape, and its articular surface is concave. The lateral plateau is more circular in outline and has a somewhat convex joint surface. The lateral plateau also overhangs the tibial shaft, especially on its posterolateral aspect, where it articulates with the fibula. Both tibial plateaus are cushioned by menisci, which deepen the articular surface. The intercondylar eminence with its medial and lateral tubercles lies in the narrow space between the two tibial plateaus. From anterior to posterior, the area of the intercondylar eminence supplies attachment to the anterior horn of the medial meniscus, distal portion of the ACL, anterior and posterior horns of the lateral meniscus, posterior horn of the medial meniscus, and proximal segment of the posterior cruciate ligament (PCL).

The patella is the largest sesamoid bone of the skeleton. It is embedded in the quadriceps femoris tendon. The anterior surface of the patella is convex and separated from the subcutaneous tissue by the prepatellar bursa. The posterior surface is divided into the medial and lateral facets by a vertical ridge that occupies the groove (trochlear notch) on the anterior surface of the femur. The lateral facet is broader and deeper. The posterior surface of the patella is covered by hyaline cartilage. The apex of the patella, which is triangular in shape and points downward, is the attachment site of the patellar ligament.

Cortical bone, because of its compact histologic composition, is devoid of signal at MRI and will appear low signal on all pulse sequences.

The medullary cavity is formed by cancellous

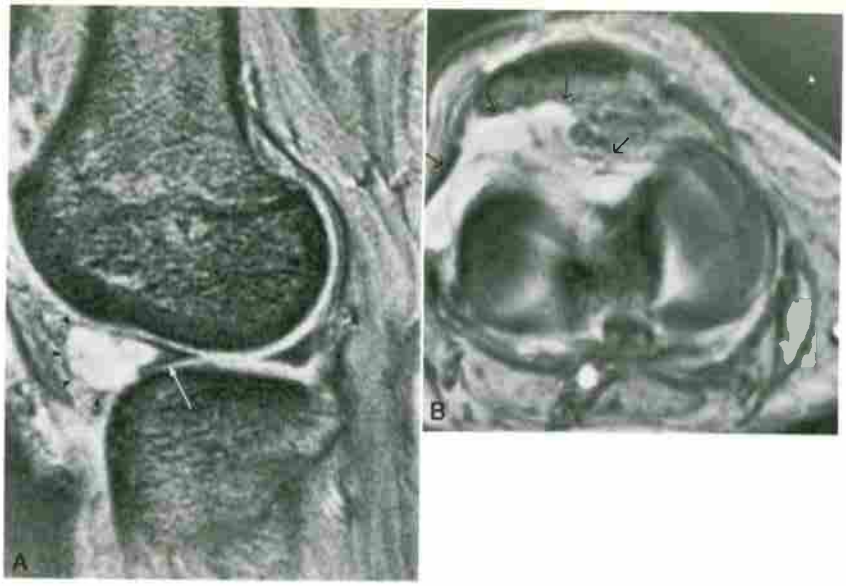

FIG 21. Meniscal cyst. **A,** Sagittal gradient-echo (TR/TE, 578/18; angle, 30 degrees) image demonstrates a horizontal cleavage tear (white arrow) of the anterior horn of the lateral meniscus in continuity with a high-signal-intensity mass (arrowheads) extending into Hoffa's fat pad, representing a meniscal cyst. **B,** Axial gradient-echo (TR/TE, 510/18; angle, 30 degrees) image shows the anterolateral extension of the cyst (arrows).

bone and marrow. In the adult, hematopoietic elements of the bone marrow have been largely replaced by fatty tissue (yellow marrow), which gives very high signal compared to bony trabeculae; thus, the final signal intensity reflects primarily the fatty marrow elements. Fatty marrow in the medullary cavity will thus have a high signal intensity similar to subcutaneous fat on all pulse sequences.

Hyaline cartilage will generally show intermediate signal intensity on spin-echo T1W sequences and low signal intensity on T2W sequences. Using the appropriate flip angle, hyaline cartilage will appear high signal on gradient-echo sequences, which contrasts with adjacent structures and may facilitate its evaluation.

MENISCI

The different roles of the menisci are to participate in load transmission, provide shock absorption, and assist in joint stability.

The medial and lateral menisci of the knee are crescent-shaped wafers of fibrocartilage. They are thicker at their peripheral (external) margins and rapidly taper to thin, free (also called inner or unattached) edges in the central region of the articulation.[16]

From birth until approximately 10 years, when the menisci have reached the adult configuration, different histologic changes occur in the menisci, including decreasing vascularity, which recedes from the center to the peripheral margin, decreasing cellularity, increasing collagen content and organization, and growth.[17] In adults, approximately 10% to 25% of the peripheral margin of the menisci is vascularized. The blood supply is derived from the genicular arteries. The peripheral zone of the menisci is also softer and innervated.

The medial meniscus is larger in diameter than the lateral meniscus and is oval. Its greatest mediolateral dimension averages 10 mm and is 3 to 5 mm thick at its periphery. The anterior horn is thinner and narrower than the posterior horn and attaches to the intercondylar eminence. The posterior horn attaches both to the intercondylar eminence and to the PCL.[17] The periphery of the medial meniscus is firmly attached to the tibia and joint capsule via the coronary ligaments and posteromedially via the posterior oblique ligament.

The lateral meniscus is nearly circular. Although it is also 3 to 5 mm thick peripherally, its width is usually greater than that of the medial meniscus, averaging 12 to 13 mm. It is also more variable in configuration than the medial meniscus, with a greater incidence of a discoid shape. The lateral meniscus is more weakly attached peripherally to the tibial plateau and joint capsule and lacks any attachment to the lateral collateral ligament because of the presence of the popliteus tendon. This results in increased mobility of the lateral meniscus and may explain in part the lower incidence of lateral tears.

Two normal structures are often present in association with menisci of the knee: the meniscofemo-

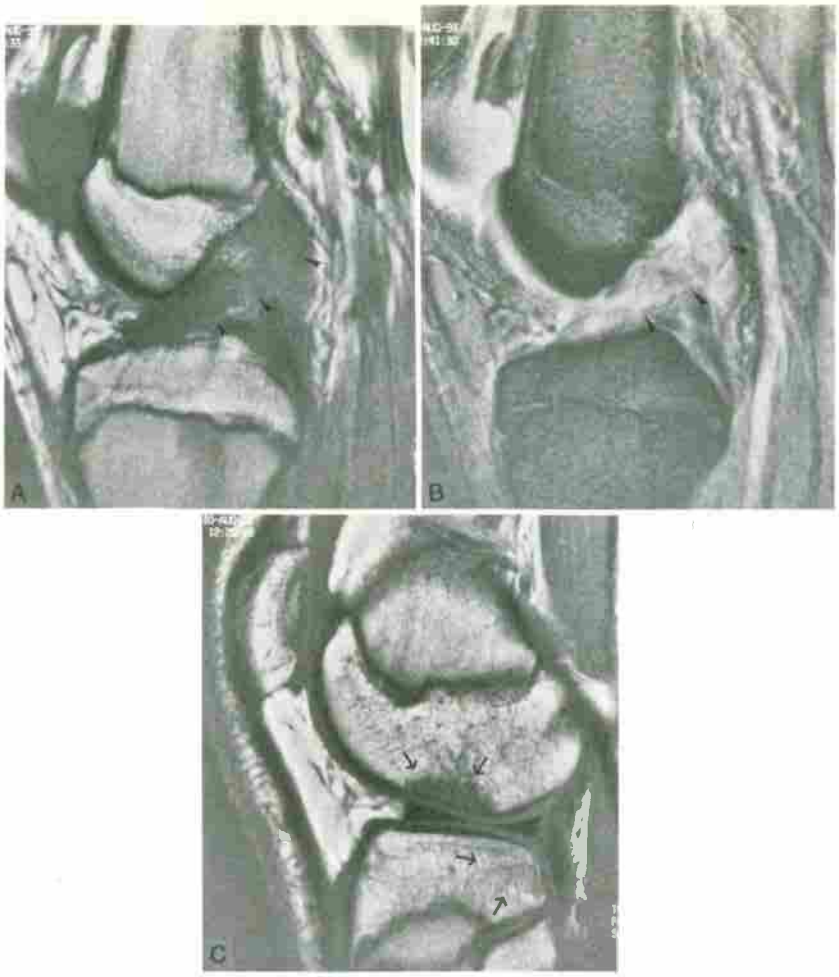

FIG 22. Acute, complete tear of anterior cruciate ligament (ACL) with bone contusions. **A,** Sagittal T1-weighted (TR/TE, 420/20) image through lateral aspect of intercondylar notch shows a mass of edema (arrowheads) in the expected location of the ACL. **B,** Corresponding gradient-echo (TR/TE, 442/18; angle, 30 degrees) sagittal image. **C,** In the same patient, sagittal T1-weighted (TR/TE, 420/20) image through the lateral joint compartment demonstrates "kissing contusions" (arrows) of the posterior aspect of the lateral tibial plateau and the lateral femoral condyle just above the anterior horn of the lateral meniscus.

ral ligaments posteriorly, and the transverse meniscal ligament of the knee anteriorly. The meniscofemoral ligament is a collection of fibers, arising from the posterior aspect of the lateral meniscus, that runs obliquely to insert on the inner surface of the medial femoral condyle. If it passes posterior to the PCL, it is known as the ligament of Wrisberg. If it passes anterior to the PCL, it is called the ligament of Humphry. These can be more easily remembered if one recalls that, from anterior to posterior, the ligaments are named alphabetically (Humphry more anterior to Wrisberg).[16] In approximately 70% of knees, one of the two ligaments will be found, whereas in 6% of knees, both are present.[17] The transverse meniscal ligament is a bundle of fibers that courses horizontally and connects the anterior convex margins of the medial and lateral menisci.

On MRI, the normal menisci, transverse meniscal ligament, and meniscofemoral ligaments demonstrate low signal intensity on all pulse sequences.

COLLATERAL LIGAMENTS

The medial (tibial) and lateral (fibular) collateral ligaments stabilize the knee by preventing hyperextension, varus, and valgus angulation of the joint. As with all other ligaments, they exhibit low signal intensity on all MR pulse sequences because they are composed of fibrous tissue, which contains few mobile protons. These ligaments are often partially or completely torn by trauma.

The medial collateral ligament (MCL) is a broad, flat band that extends between the medial epicondyle of the femur and the tibia. It consists of a long

FIG 23. Chronic anterior cruciate ligament (ACL) tear. Sagittal T1-weighted (TR/TE, 600/20) image through lateral aspect of intercondylar notch shows the ACL fibers (arrows) with an abnormal, near horizontal course. Also, the proximal end of the tendon does not extend to its expected femoral insertion, and appears scarred down to the posterior cruciate ligament (PCL). Note the absence of edema and the abnormal wavy contour of the ACL fibers.

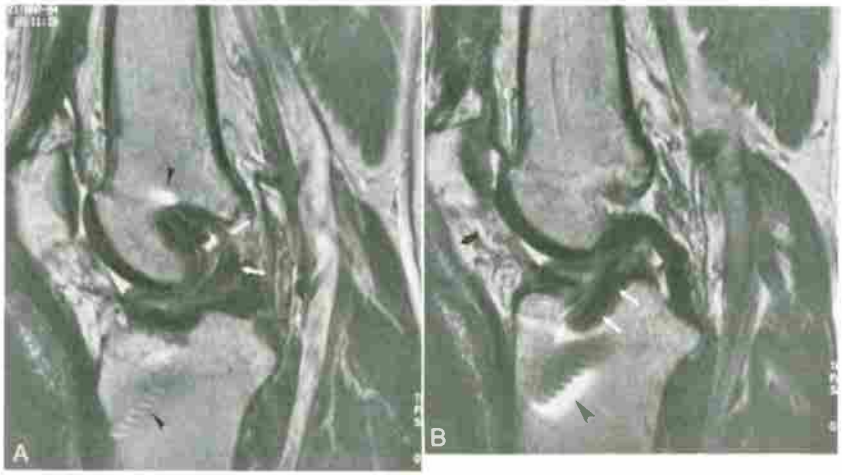

FIG 24. Intact anterior cruciate ligament (ACL) graft. **A, B,** Sagittal T2-weighted (TR/TE, 2500/80) images through the intercondylar notch. The low-signal-intensity ACL graft (white arrows) can be pieced together on two adjacent sections. The bone–tendon–bone ACL graft is secured in the tibial and femoral tunnels with interference screws, which create metallic artifacts (arrowheads). The proximal patellar tendon (black arrow) is thinned and demonstrates high signal intensity where the graft was harvested. Note that the tibial tunnel orientation is slightly posterior and almost parallel to the roof of the intercondylar notch.

superficial layer and a shorter deep layer. The former attaches to the tibial shaft approximately 5 cm below the joint line, and the latter attaches to the medial tibial plateau and medial meniscus. The deep portion of the ligament really represents an area of thickening of the joint capsule. A small bursa with surrounding high-signal-intensity fat lies between the superficial and deep capsular layers of the MCL and must not be misinterpreted as a meniscocapsular separation.

Anteriorly, the ligament blends with the medial patellar retinaculum. In addition, it is crossed below by the tendons of the pes anserinus muscles (sartorius, gracilis, and semitendinosus) with the anserine bursa being interposed. Posteriorly, the ligament blends with the capsule.

The lateral collateral ligament (LCL) is a strong, rounded cord that is entirely separate from the capsule of the knee joint. It is attached above to the lateral epicondyle of the femur, immediately above and behind the groove for the tendon of the popliteus muscle and, below, to the head of the fibula, approximately 1 cm anterior to its apex. The popliteus tendon passes deep to the ligament with a small bursa interposed between the two structures. Deep to the ligament run the lateral geniculate ves-

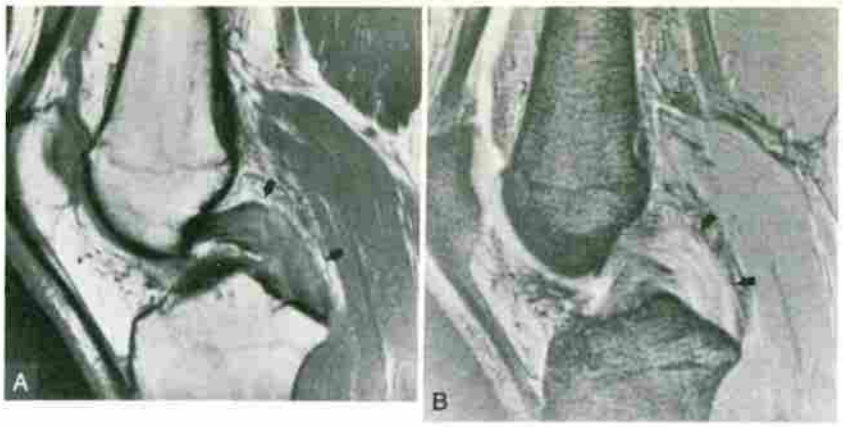

FIG 25. Acute complete posterior cruciate ligament (PCL) rupture. **A,** Sagittal T1-weighted (TR/TE, 800/20) image through PCL demonstrates interruption of the fibers and replacement by a mass of edema and hemorrhage (arrows). **B,** Corresponding sagittal gradient-echo (TR/TE, 550/20; angle, 30 degrees) image.

sels and nerve. The biceps femoris tendon attaches on the apex of the fibular head and is separated from the fibular ligament by a small bursa. More anteriorly on the lateral side of the knee is the iliotibial band, which curves over the lateral patellar retinaculum and blends with the capsule just below the articular surface of the tibia, on Gerty's tubercle.

Another structure contributing to the stability of the knee on the lateral side is the arcuate popliteal ligament, which runs from the posterior border of the intercondylar area of the tibia, obliquely and laterally, to insert on the fibular head. It passes over the popliteus muscle.

ANTERIOR CRUCIATE LIGAMENT

The ACL is a very important stabilizing structure of the knee. It is a band of dense connective tissue that has its tibial attachment on the intercondylar eminence, lateral and slightly posterior to the anterior horn of the medial meniscus. It extends superiorly and laterally in the intercondylar notch and inserts distally on the posterior aspect of the intercondylar surface of the lateral femoral condyle.[14,15] Frequently, part of its tibial attachment blends into the anterior horn of the lateral meniscus. The tibial insertion of the ACL is larger and stronger than its femoral attachment. In adults, the ACL averages 4 cm in length and 1 cm in width. The ACL is an intraarticular, extrasynovial (being completely invested in reflections of the synovium) structure composed of two distinct fascicles, the anteromedial and posterolateral bundles. The former is taut in flexion, and the latter is tense mainly in extension. The ACL has five major functions in the knee: it (1) resists anterior tibial translation on the femur in flexion, (2) prevents hyperextension of the joint, (3) assures rotatory knee control, (4) assists in restraining valgus and varus forces, and (5) helps stabilize the knee near full extension.[18]

POSTERIOR CRUCIATE LIGAMENT

The PCL is shorter but thicker and stronger than the ACL. It originates on the posterior intercondylar area of the tibia, well below the tibial articular margin, sometimes as much as 2 cm below the joint line. Part of its tibial attachment blends with the posterior horn of the lateral meniscus. In the intercondylar notch, its course is less oblique than that of the ACL. From its proximal tibial insertion, it extends superiorly, at first in the anatomic sagittal plane close to the vertical plane, and then almost abruptly changes orientation and becomes more horizontal to attach to the middle and anterior portion of the lateral surface of the medial femoral condyle, near the roof of the intercondylar notch.[14,15] The PCL is tightest in full flexion. It provides 95% of the total restraint to posterior translation of the knee and assists in restraining varus and valgus movements.[19] In the intercondylar notch, the PCL is medial to the ACL and is also an intracapsular, extrasynovial structure.

QUADRICEPS AND PATELLAR TENDONS

The quadriceps femoris muscle is the unification of four muscle bundles, the rectus femoris, vastus lateralis, vastus intermedius, and vastus medialis, which arise separately but converge to a single tendon made of different layers. The quadriceps tendon is formed primarily by the rectus femoris ten-

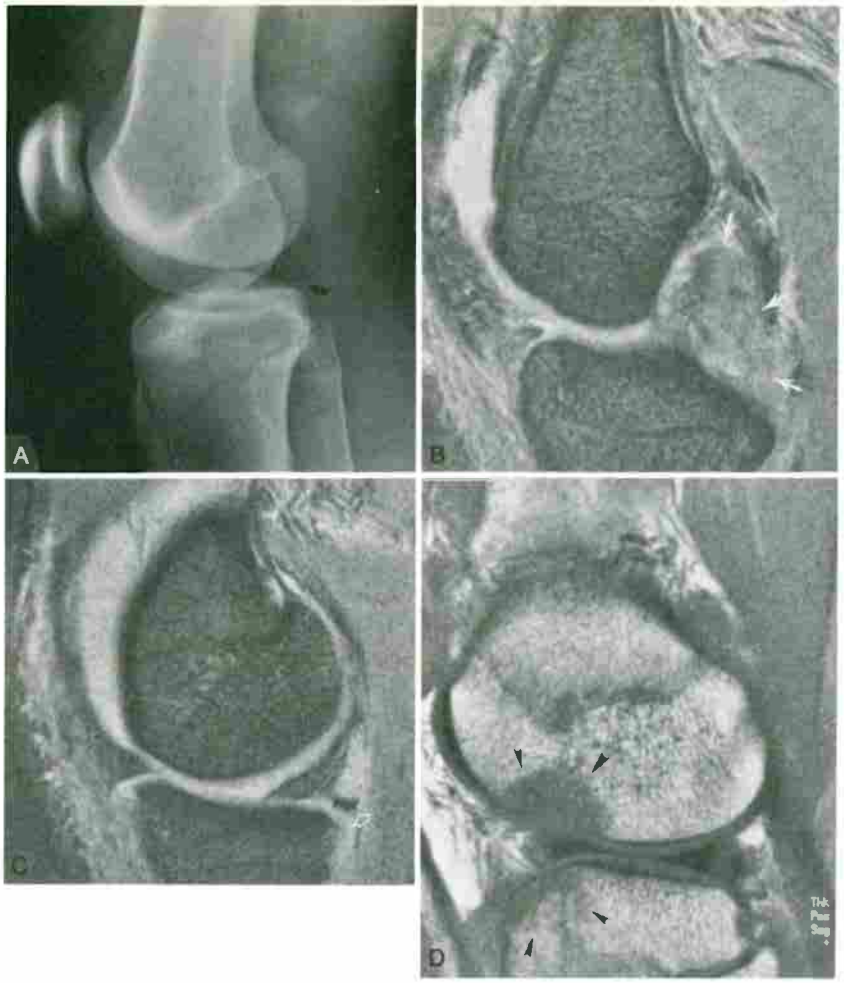

FIG 26. Complete tear of posterior cruciate ligament (PCL) with avulsion fracture at the tibial insertion site. **A,** Lateral radiograph of the knee demonstrates a joint effusion (asterisk) and a subtle fleck of bone (black arrow) adjacent to the posterior tibial rim. Sagittal gradient-echo (TR/TE, 442/18; angle, 30 degrees) images through the intercondylar notch **(B)** and through the lateral aspect of the medial joint compartment **(C)** show a cloud of edema and hemorrhage (white arrows) without recognizable ligamentous fibers in the expected course of the PCL and the small avulsion fracture (open white arrow) off the tibial attachment of the PCL. **D,** Sagittal T1-weighted (TR/TE, 430/20) image through the lateral joint compartment demonstrates femoral impaction fracture and bone contusion (arrowheads) of the anterior aspect of the lateral femoral condyle and lateral tibial plateau resulting from the hyperextension injury.

don and inserts on the superior pole of the patella. On MRI, the quadriceps tendon will often demonstrate a striated appearance with alternating areas of linear low and intermediate signal intensity running longitudinally in the tendon. These striations are caused by the longitudinal arrangement of coarse fascicles of collagen. Both the vastus medialis and vastus lateralis also contribute to form the quadriceps tendon, but in addition, they extend peripherally to form the medial and lateral retinacula, respectively, which blend with and reinforce the joint capsule. The vastus intermedius tendon fibers end in a superficial aponeurosis, which blends with the deep surface of the other three muscle tendons. The suprapatellar bursa, which is freely in communication with the articular cavity, is interposed between the quadriceps tendon and the anterior surface of the distal femur.

The patellar tendon is the continuation of the central portion of the quadriceps tendon, which extends from the patella to the tibial tuberosity. It is a very strong, flat band, approximately 8 cm long, which courses somewhat obliquely downward to its tibial insertion. The deep infrapatellar bursa is interposed between the distal tendon and underlying tibial tuberosity, whereas superiorly, the infrapatellar fat pad (Hoffa fat pad) intervenes between the tendon and the synovial membrane.

The appearance of tendons on MRI can be explained by their biochemical structure. Tendons

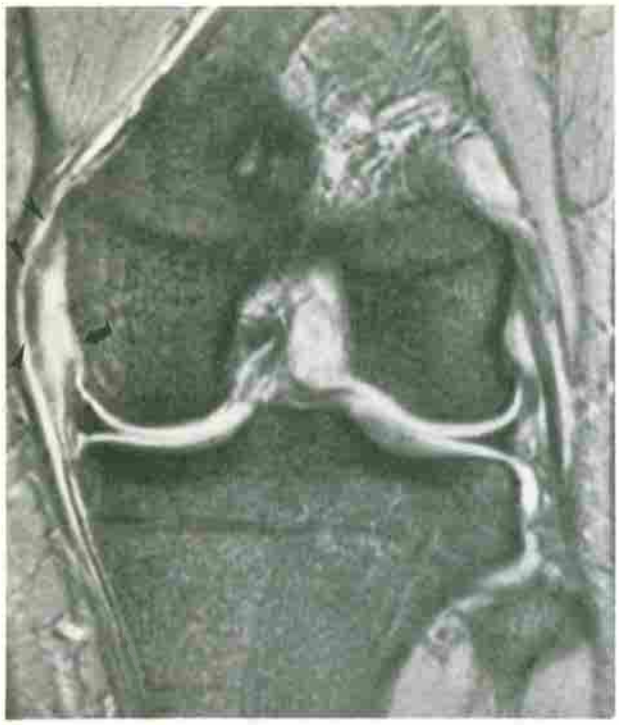

FIG 27. Partial tear of medial collateral ligament (MCL). Coronal gradient-echo (TR/TE, 578/18; angle, 30 degrees) image shows thickening and high signal intensity of the proximal MCL (arrowheads) as well as disruption of the deep fibers at the femoral attachment (arrow) from a partial MCL tear. Also note the high signal intensity surrounding edema.

FIG 28. Complete medial collateral ligament (MCL) tear. Coronal T1-weighted (TR/TE, 700/16) image demonstrates complete tear of the MCL at the distal insertion (arrow) resulting from a valgus force with associated large bone contusions (arrowheads) of the lateral compartment. The MCL is separated from the underlying meniscus and surrounded by edema.

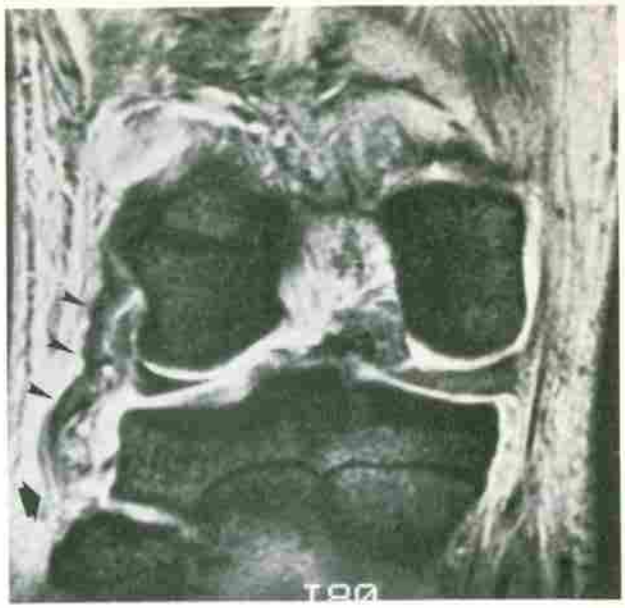

FIG 29. Complete lateral collateral ligament (LCL) tear. Coronal gradient-echo (TR/TE, 533/20; angle, 30 degrees) image demonstrates undulation and thickening of the LCL (arrowheads). The ligamentous rupture has occurred near the distal insertion on the fibular head (arrow). Note the surrounding high-signal-intensity soft-tissue edema/hemorrhage.

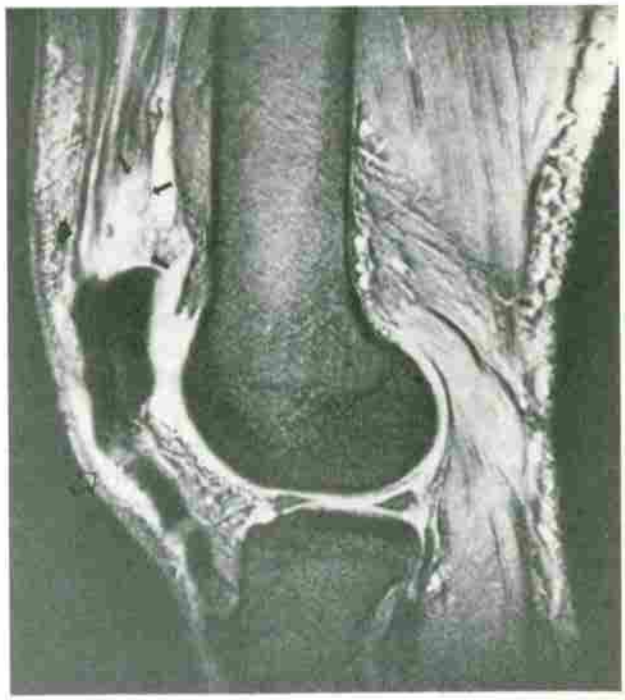

FIG 30. Partial quadriceps tendon tear. Sagittal gradient-echo (TR/TE, 442/18, angle, 30 degrees) image shows disruption of many layers of the tendon with replacement by high-signal-intensity edema and hemorrhage (thin arrows). The most anterior tendon layer (thick arrow) originating from the rectus femoris muscle remains intact. Note the undulating patellar tendon owing to the quadriceps tendon pathology. A joint effusion as well as a posttraumatic prepatellar bursitis (open arrow) are present.

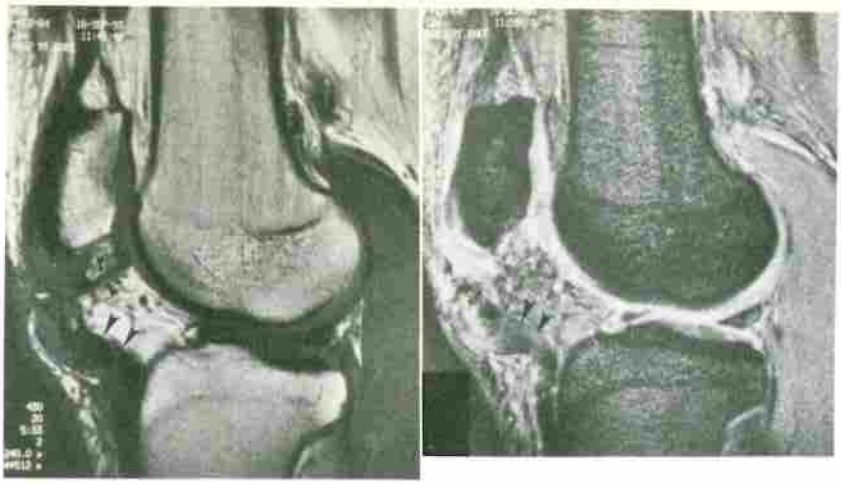

FIG 31. Acute patellar tendon rupture. The proximal patellar tendon ruptured spontaneously during a football game. **A,** Sagittal T1-weighted (TR/TE, 430/20) and **(B)** gradient-echo (TR/TE, 442/18; angle, 30 degrees) images show complete disruption of the tendon fibers (arrowheads) with retraction of the tendon. There is a mass of edema and hemorrhage at the site of rupture inferior to the patella. There is also traumatic disruption of the infrapatellar fat pad, best demonstrated on the T1-weighted image (small arrows). Also note a small bone fragment avulsed from the inferior pole of the patella (open arrow).

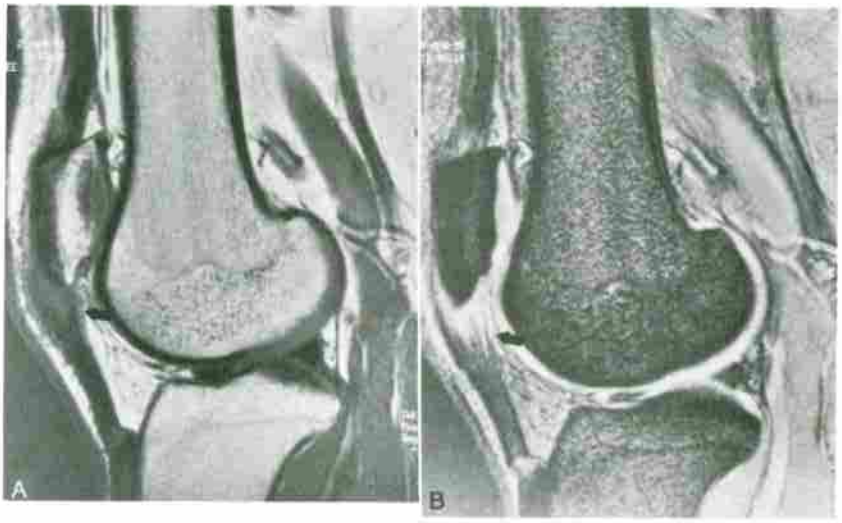

FIG 32. Jumper's knee. **A,** Sagittal T1-weighted (TR/TE, 430/20) and **(B)** corresponding gradient-echo (TR/TE, 442/18; angle, 30 degrees) images demonstrate abnormal thickening and high signal intensity in the proximal patellar tendon from partial tears (arrow).

are relatively avascular structures composed predominantly of collagen and, to a lesser extent, elastin, reticulin fibers, and tenocytes embedded in an amorphous ground substance. The tensile strength of tendons comes mainly from the collagen fibers, which are arranged in a parallel pattern. Collagen fibers are formed from smaller fibrils, which are made of even smaller microfibrils. Collagen microfibrils are composed of a protein, tropocollagen, which consists of three polypeptide chains arranged in a triple-helix configuration that tightly binds water molecules. Thus, even though tendons are composed largely of water, the lack of rotational motion of the water molecules held within the triple helix of the protein that forms collagen results in tendons (as well as ligaments and menisci, for the same reasons) that have extremely low signal intensity on MRI on all pulse sequences.[16]

JOINT CAPSULE AND SURROUNDING STRUCTURES

The fibrous articular capsule is a complex structure, inherently weak, but reinforced by surrounding ligaments and tendon aponeuroses with which it is intimately intermixed. On the posterior aspect of the knee, the capsular fibers are anchored superiorly on the margins of the femoral condyles and

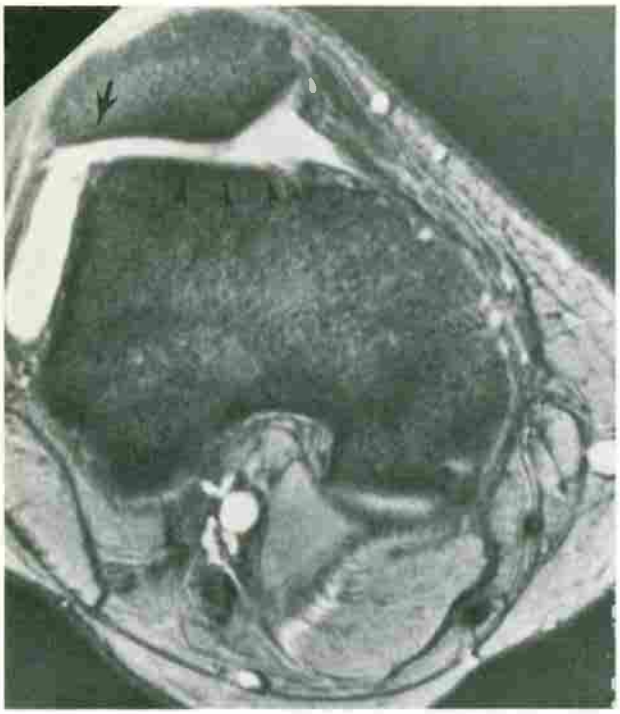

FIG 33. Patellar tracking abnormality. Gradient-echo (TR/TE, 600/18; angle, 30 degrees) axial image shows lateral subluxation of the patella (arrow). The patellar tilt angle measures 4 degrees. Also note the shallow trochlear groove (arrowheads). A joint effusion is also present.

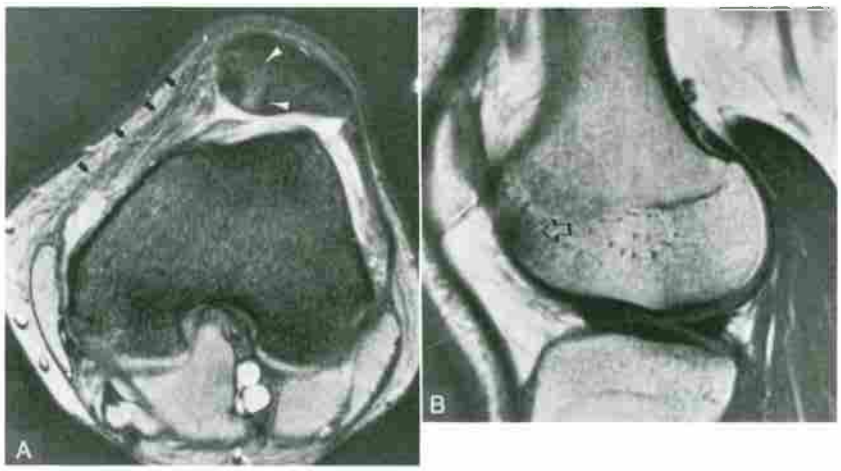

FIG 34. Sequelae of patellar dislocation. **A,** Axial gradient-echo (TR/TE, 578/18; angle, 30 degrees) image demonstrates a contusion of the medial facet of the patella (white arrowheads), resulting from the impaction against the lateral femoral condyle. The medial retinaculum (arrows) shows diffuse high-signal-intensity separating fibers representing partial tears. Also note the lateral subluxation of the patella. **B,** Sagittal T1-weighted (TR/TE, 430/20) image through the lateral joint compartment shows the bone contusion of the anterior aspect of the lateral femoral condyle (open arrow).

inferiorly attach to the margins of the tibial plateaus. On the anterior aspect of the knee, the capsule inserts superiorly to the patella, and extends inferiorly, blending with the posteromedial and posterolateral retinacula.

The oblique popliteal ligament, which originates from the semimembranosus tendon, and the arcuate popliteal ligament are two small structures contributing strength to the capsule posteriorly. These small ligaments cannot be seen on a knee MRI study.

Other external structures reinforcing the capsule are, on the lateral side, the biceps femoris tendon, iliotibial band, popliteus tendon, and LCL, and on the medial side, the tendons of the pes anserinus muscle, semimembranosus tendon, and MCL.

In the popliteal fossa, adjacent to the fibrous capsule and the two heads of the gastrocnemius

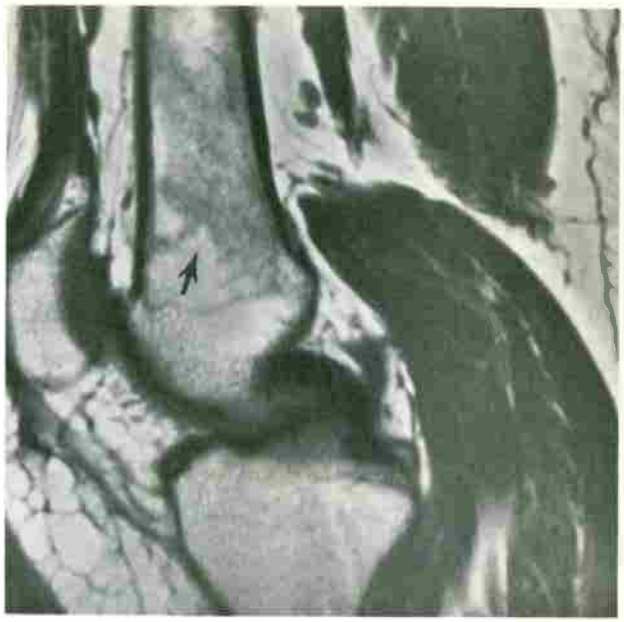

FIG 35. Hematopoietic hyperplasia in obese 38-year-old woman. Sagittal T1-weighted (TR/TE, 430/20) image through intercondylar notch. Note the confluent areas of intermediate signal intensity in distal diametaphysis of femur, representing red marrow expansion (arrow). The process is not seen in the proximal tibia.

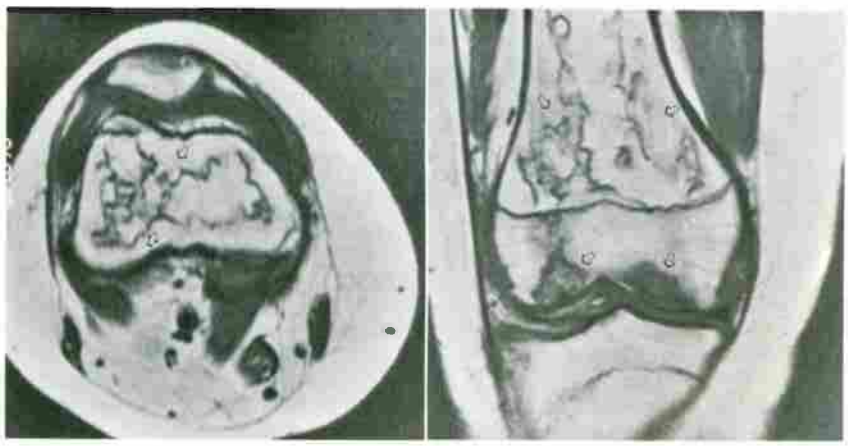

FIG 36. Medullary infarcts. **A,** Axial and **(B)** coronal T1-weighted (TR/TE, 500, 700/20) images. This 16 year old with Hodgkin's disease developed knee pain after bone marrow transplant. Characteristic appearance of metaphyseal and epiphyseal infarcts with low-signal-intensity serpiginous margins (arrows).

muscle, lie the popliteal vessels. The popliteal vein runs medially to the artery. The popliteal artery is often accompanied by lymph nodes, especially in young individuals. These are commonly seen at MRI and appear as small oval structures with intermediate signal intensity on T1W sequences and high signal intensity on gradient-echo or T2W sequences. The tibial nerve also runs in the popliteal fossa immediately posterior to the popliteal artery and vein.

Multiple bursae are found around the knee joint, interposed between structures that move relative to one another. Their purpose is to alleviate friction by creating a space between two tightly apposed structures. Bursae are small pouches lined by synovium and normally contain an imperceptible film of synovial fluid. Some bursae communicate with the knee joint. Bursae are not normally seen on MRI except when they become pathologically filled with fluid; then they are seen as low-signal-intensity structures on T1W sequences and high signal intensity on T2W or T2* sequences. Knowledge of the location of bursae facilitates the diagnosis of bursitis.

There are four bursae in the anterior aspect of the knee: (1) the subcutaneous prepatellar bursa interposed between the lower part of the patella and the skin; (2) the deep infrapatellar bursa between the tibia and distal patellar tendon; (3) the subcutaneous infrapatellar bursa between the inferior aspect

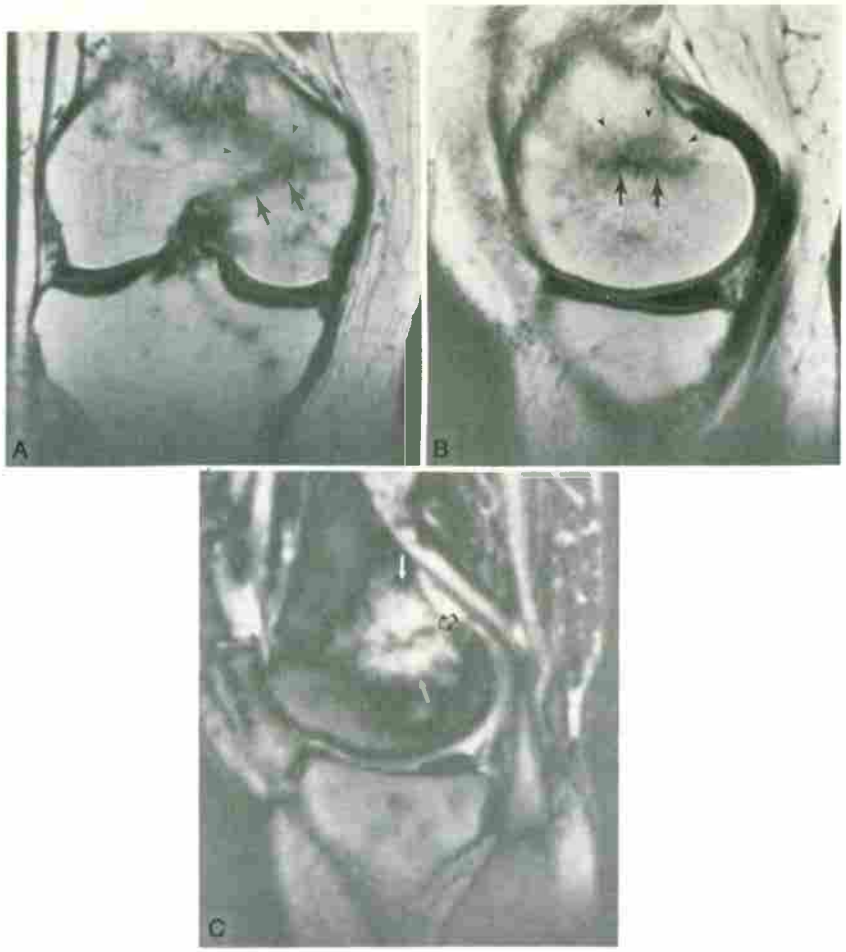

FIG 37. Insufficiency fracture. This elderly woman complained of knee pain approximately 2 months after undergoing a left total hip replacement. **A,** Coronal and **(B)** sagittal T1-weighted (TR/TE, 430/20) images demonstrate a low-signal linear insufficiency fracture (arrows) of the medial femoral condyle. Surrounding edema (arrowheads) appears as a more diffuse, ill-defined low-signal-intensity pattern. **C,** Sagittal STIR (TR/TE,TIR1, 3600/19, 150) image again shows the linear insufficiency fracture (open arrow). Note the increased conspicuity of surrounding marrow edema on STIR images, which appears as diffuse confluent high signal intensity (white arrow).

of the tibial tuberosity and the skin; and (4) the suprapatellar bursa, which communicates with the knee joint and is interposed between the prefemoral and suprapatellar fat pads.

There are also four bursae on the lateral aspect of the knee: one that sometimes communicates with the joint cavity is located underneath the lateral head of the gastrocnemius; two more are found on each side of the fibular collateral ligament, creating a space between the popliteus tendon and biceps femoris tendon, respectively; the fourth bursa is interposed between the popliteus tendon and lateral femoral condyle.

On the medial aspect of the knee, four bursae can be found: (1) the anserine bursa separating the MCL and the tendons of the pes anserinus muscles; (2) a second bursa between the medial head of the gastrocnemius and the joint capsule; (3) the gastrocnemius–semimembranosus bursa between the semimembranosus tendon and medial head of the gastrocnemius; and (4) a bursa deep to the MCL.[15]

A SYSTEMATIC APPROACH TO INTERPRETATION OF KNEE MRI

It is imperative to develop a systematic approach to reading a knee MRI examination that will ensure a thorough evaluation. In addition, using a constant, reproducible diagnostic method increases the reader's awareness of abnormalities.

The survey begins with evaluation of the sagittal images. The menisci are assessed primarily in the sagittal plane. Moving from the periphery toward the intercondylar notch, the lateral and medial menisci show a "bow-tie" appearance that is formed by the triangular-shaped anterior and posterior

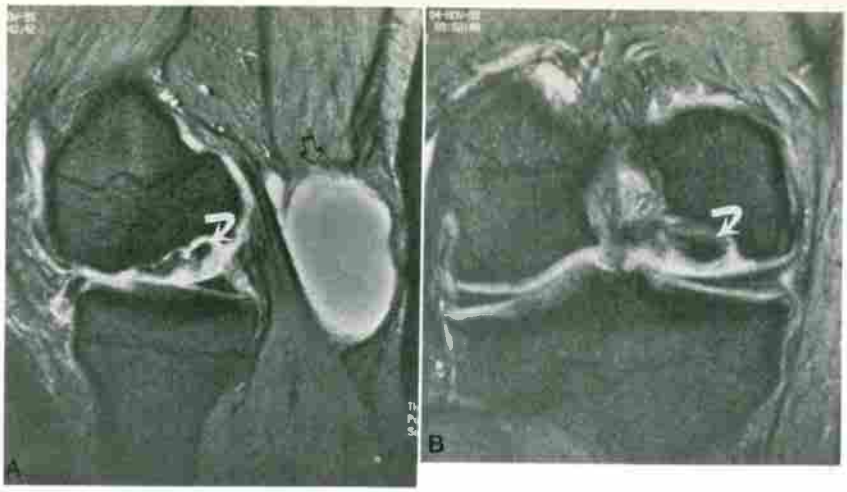

FIG 38. Osteochondritis dissecans. **A,** Sagittal and **(B)** coronal gradient-echo (TR/TE, 578/18; angle, 30 degrees) images demonstrate an area of osteochondritis dissecans (curved arrow) on the lateral aspect of the medial femoral condyle. The osteochondral fragment is low signal intensity and is separated from the parent bone by high signal intensity, which can represent either insinuating joint fluid or granulation tissue. Note the large popliteal cyst (open arrow).

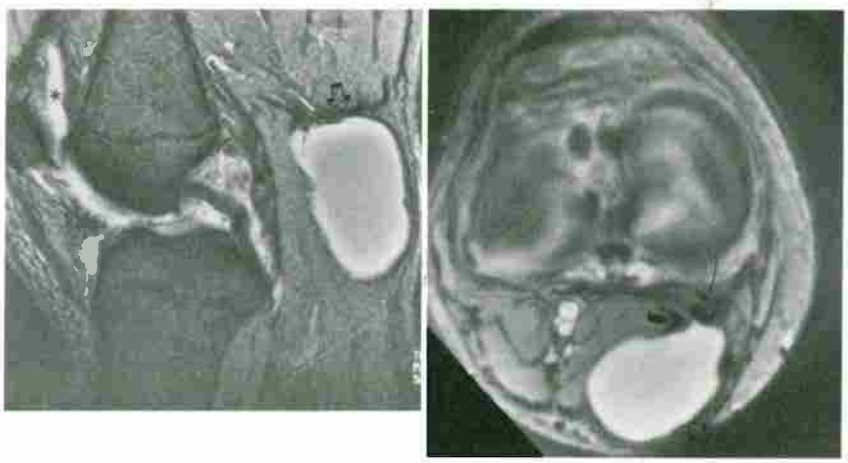

FIG 39. Popliteal cyst. Gradient echo **(A)** sagittal (TR/TE, 442/18, angle, 30 degrees) and **(B)** axial (TR\TE, 510\18; angle, 30 degrees) images demonstrate an extracapsular high-signal-intensity cystic mass (open arrow). The cyst communicates with the joint through a small channel between the tendons of the semimembranosus muscle (long arrow) and medial head of the gastrocnemius muscle (thick arrow). Note also the presence of a joint effusion (asterisk).

horns of the meniscus and the intervening body of the meniscus. This bow-tie configuration formed by the continuity of the meniscus between the anterior and posterior horns should be seen on two adjacent images if 4 or 5 mm thick sections are obtained, owing to the fact that the average width of the body of the meniscus in its mediolateral dimension is 11.6 mm. The height of a meniscus rapidly diminishes from its periphery to its free edge, so that the body (middle of the bow-tie) should be obviously of different thickness on the two adjacent sagittal cuts where it is present. These concepts are important when diagnosing bucket-handle tears and discoid menisci.[16]

The lateral and medial menisci appear as two separate triangular structures near the intercondylar notch, representing the anterior and posterior horns. The lateral meniscus has anterior and posterior horns of similar size. The medial meniscus has a posterior horn approximately twice as large in anteroposterior dimension as its anterior horn. One can easily determine if the medial or lateral aspect of the knee is being examined by the configuration of the tibia as well as that of the menisci. Recall that the medial plateau is slightly concave and symmetric, whereas the lateral tibial plateau has a flat or convex articular surface and is asymmetric with a large posterior projection (Figs. 1 and 2).

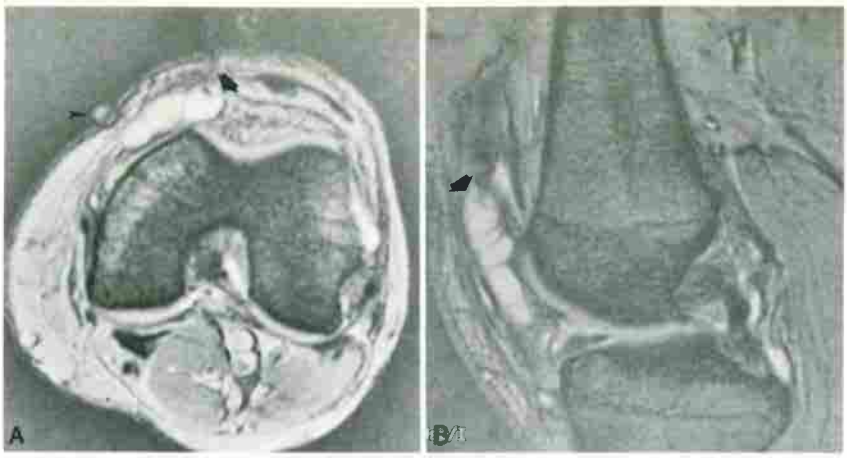

FIG 40. Ganglion cyst arising in medial patellar retinaculum. **A,** Axial and **(B)** sagittal gradient-echo (TR/TE, 483/20; angle, 30 degrees) images demonstrate a cystic mass (arrow) with internal low-signal-intensity septations. A marker was placed on the skin (arrowhead) where a mass was felt.

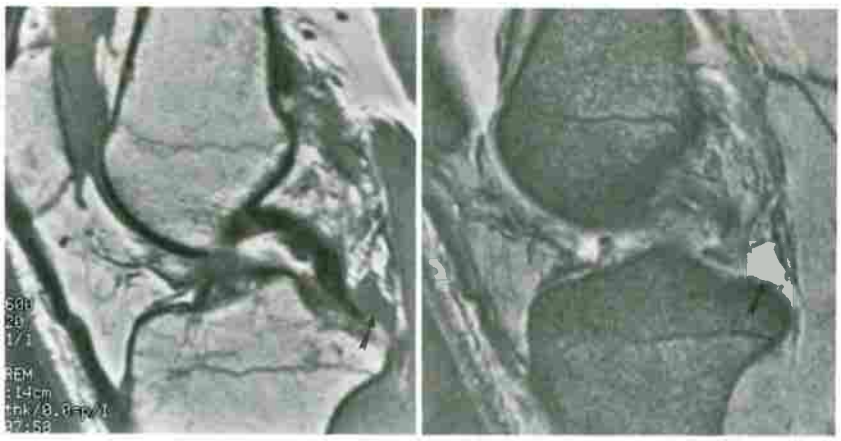

FIG 41. Sagittal **(A)** T1-weighted (TR/TE, 600/20) and corresponding **(B)** gradient-echo (TR/TE, 483/20; angle, 30 degrees) images. Ganglion cyst arising from the tibial insertion of the posterior cruciate ligament (arrow) appears as a low-signal-intensity, well-circumscribed mass on the T1-weighted image and shows homogeneous increased signal intensity on the gradient-echo image.

The menisci should have a homogeneous low signal intensity or may be seen with intrasubstance high signal intensity that does not extend to the joint margins. This finding is not of clinical significance.

After examination of the menisci in the sagittal plane, we proceed with the evaluation of the cruciate ligaments. Again, these are primarily assessed on the sagittal images. The ACL should appear as a low-signal or striated (parallel high and low signal, mainly in its distal portion) band-like structure extending from the top of the intercondylar notch in its lateral aspect, coursing distally and anteriorly to the tibial plateau at an angle parallel to or slightly steeper than the cortical roof (approximately 45° angle to the tibial plateau) of the intercondylar notch. The ligament appears as a taut and relatively straight band-like structure. If not seen in its entirety on a single image, it can be pieced together on two adjacent images (Fig. 3).

The PCL is readily assessed on sagittal images.[20] Being thicker than the ACL and because of its almost direct anteroposterior course in the intercondylar notch, it can normally be seen in its entirety at least on one sagittal cut. It originates on the posterior aspect of the intercondylar eminence and extends superiorly and anteriorly to insert on the medial femoral condyle. It is convex posteriorly, and its appearance has been likened to that of a boomerang[21] (Fig. 4).

The quadriceps and patellar tendons are evaluated on sagittal images and are low-signal, band-like structures except for the distal segment of the quadriceps tendon, which normally presents a laminated appearance. This multilayered appearance is the result of the disposition of the four

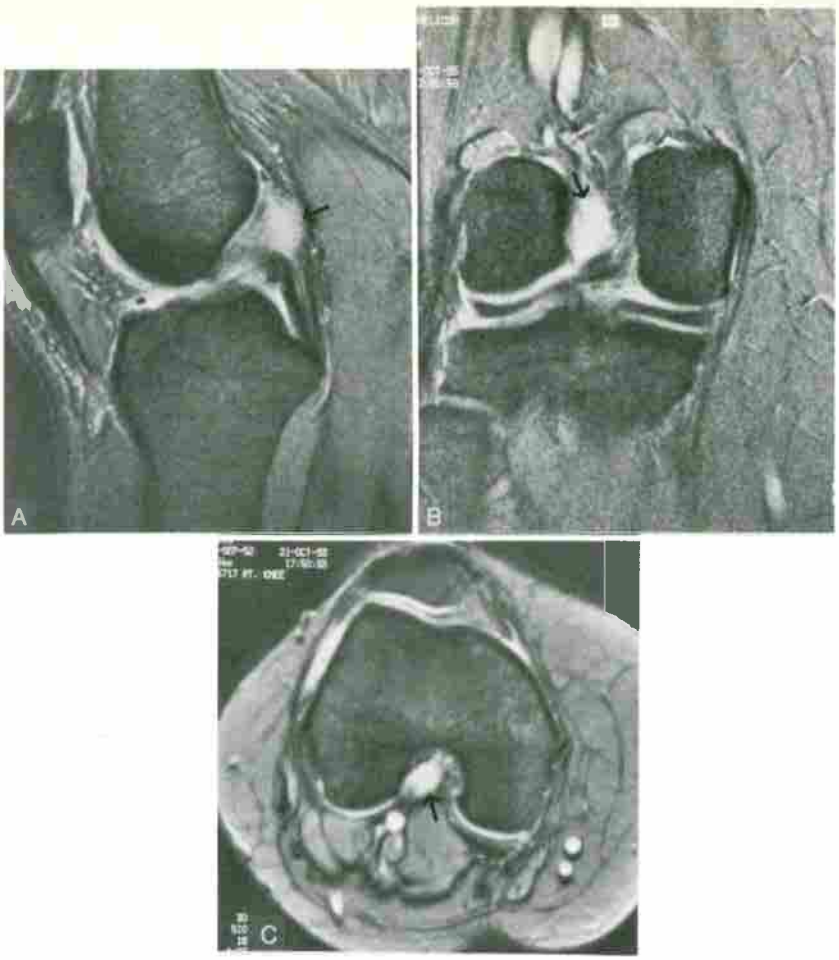

FIG 42. A, Sagittal, **(B)** coronal, **(C)** axial gradient-echo (TR/TE, 510/18; angle, 30 degrees) images. Multiplanar demonstration of a ganglion cyst (arrow) arising from the femoral attachment of the ACL.

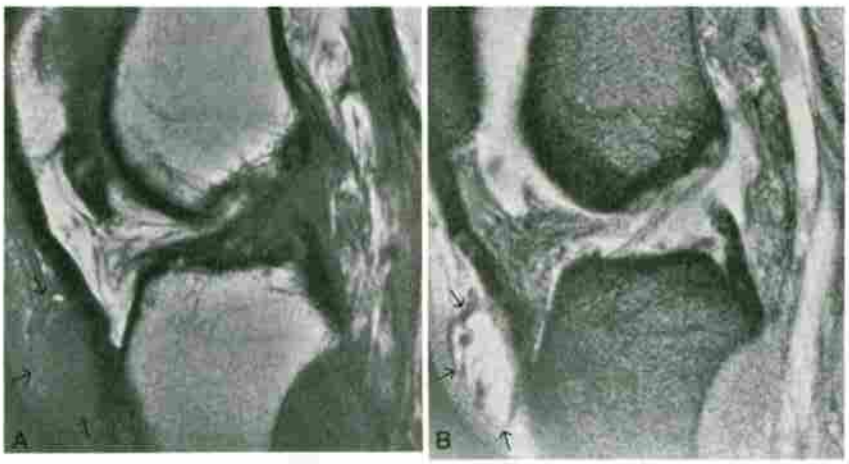

FIG 43. Superficial infrapatellar bursitis (arrows). **A,** Sagittal T1-weighted (TR/TE, 430/20) and **(B)** gradient-echo (TR/TE, 442/18; angle, 30 degrees) images.

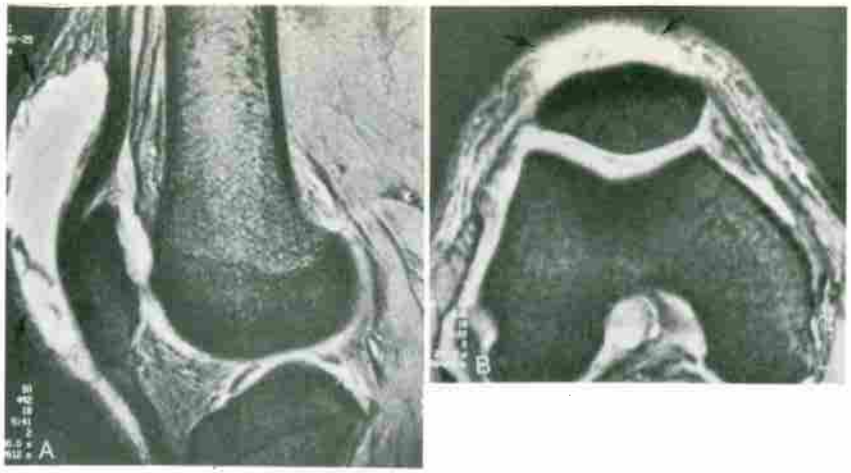

FIG 44. Prepatellar bursitis (arrows). **A,** Sagittal and **(B)** axial gradient-echo (TR/TE, 442/18; angle, 30 degrees) images.

quadriceps muscles. Each muscle may potentially give a separate layer to the tendon. One study showed that most tendons (86%) are composed of either two or three layers.[22]

The most superficial layer arises from the rectus femoris and the deepest layer from the vastus intermedius. The vastus medialis and vastus lateralis muscles may form a separate third layer or blend in with the superficial and deep layer to form a two-layered tendon. The quadriceps and patellar tendons are of uniform thickness with parallel margins.

The osseous structures are best evaluated on sagittal T1W images. The integrity of the articular surfaces and the signal intensity of the bone marrow are assessed. In adults, the medullary cavity is composed mainly of fatty marrow and thus shows predominantly high signal intensity on T1W sequences. Areas of hematopoietic (red) marrow are often normally seen in the diametaphysis of the distal femur and proximal tibia as intermediate signal intensity on T1W images.

Finally, the soft tissues surrounding the knee are examined for the presence of any abnormal signal intensity or masses.

Coronal images are evaluated next. The primary value of the coronal images is in evaluation of the collateral ligaments. This is also a valuable plane for confirming abnormalities of menisci, cruciate ligaments, and osseous structures suspected on the sagittal images.

Reviewing the images sequentially from back to front, on the lateral aspect of the knee, one should identify and assess the integrity of the biceps femoris tendon, LCL, and iliotibial band. These should appear as low-signal-intensity, band-like structures (Fig. 5). The surrounding soft tissues are evaluated for evidence of edema or masses. On the medial aspect of the knee, approximately at the level of the intercondylar tubercles, the MCL is best seen. The superficial and deep layers of the MCL can be seen as two linear, relatively thin, low-signal-intensity bands bridging the joint line. They can normally be separated by a small amount of fat, which will appear high signal intensity and should not be misinterpreted as edema. The deep layer of the MCL extends from the medial femoral epicondyle to the tibial plateau, whereas the superficial layer extends down to the tibial shaft as far as 5 cm below the joint line (Fig. 6).

The ACL is also evaluated on coronal views. On sequential coronal images, in the lateral aspect of the intercondylar notch, the intact ACL appears as a low-signal linear band coursing obliquely from its femoral insertion to its tibial attachment. Its distal segment often shows a striated appearance. Although the PCL is best evaluated on sagittal images, its horizontal portion is also assessed on coronal views, which sometimes helps to confirm a diagnosis. On coronal images, the PCL appears as a low-signal round structure in the medial side of the intercondylar notch.

Finally, the axial images are reviewed, with particular attention to the patellofemoral joint and the soft-tissue structures in the popliteal fossa (Fig. 7). In addition, the anatomy of the cruciate and collateral ligaments is again evaluated. On sequential axial images, the normal ACL appears as an oval structure of low signal intensity in the lateral aspect of the intercondylar notch. The proximal vertical segment of the PCL is seen in cross-section as a round low-signal-intensity structure in the medial aspect of the intercondylar notch. The MCL

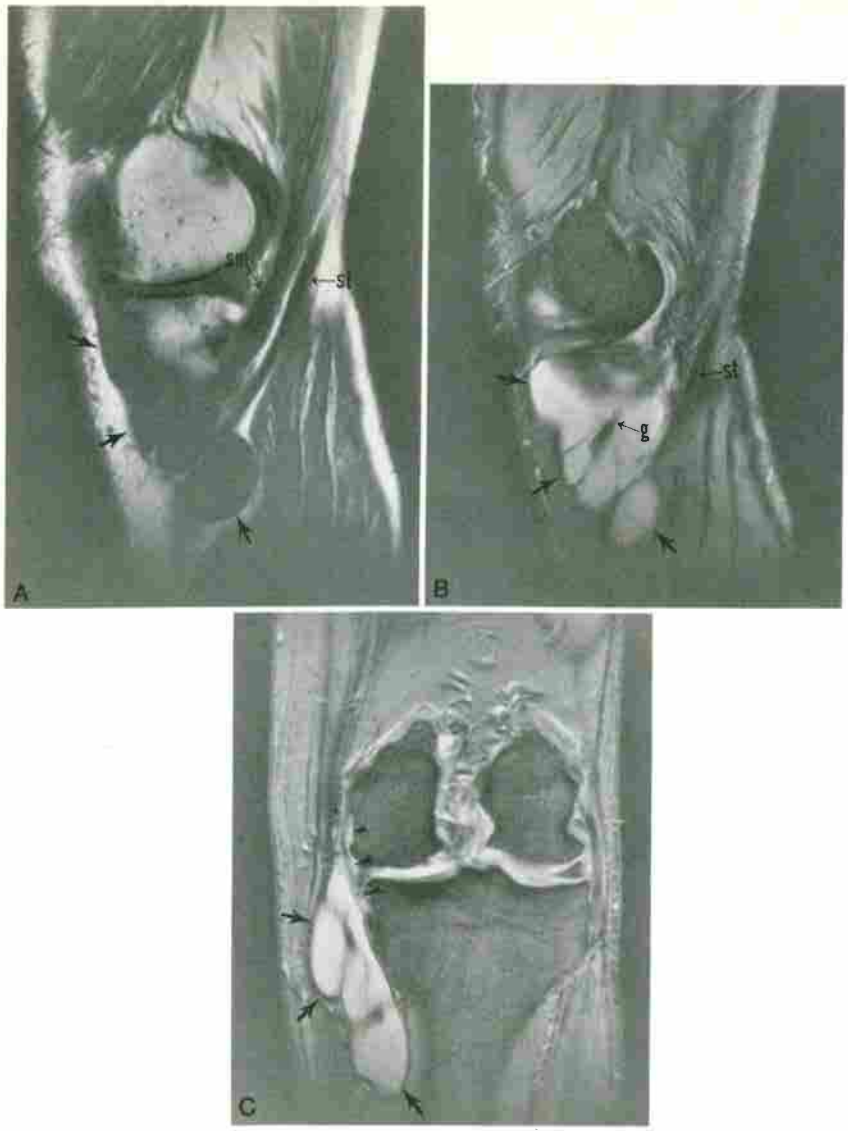

FIG 45. Anserine bursitis. **A,** Sagittal T1-weighted (TR/TE, 600/20), and **(B)** gradient-echo (TR/TE, 600/18; angle, 30 degrees) images through peripheral aspect of medial joint compartment show intermediate-intensity and high-intensity lobulated mass (arrows) deep to the semitendinosus (st) and gracilis (g) tendons, respectively. **C,** Coronal gradient-echo (TR/TE, 600/18; angle, 30 degrees) image shows the lesion (arrows) to be superficial to the MCL (arrowheads). The medial meniscus is absent, and there is moderate degenerative joint disease of the medial compartment. Semimembranosus tendon (sm).

and LCL are also seen in cross section on each side of the knee.

Multiplanar assessment of the anatomic structures of the knee can help clarify a diagnosis.[23] One very important concept to keep in mind while reviewing a knee MRI study is the mechanism of injury. Finding an abnormality and knowing how the injury might have occurred should prompt an intended search for associated injuries. The association of ACL tears and bone contusions of the posterior lateral tibial plateau and of the anterior lateral femoral condyle is one example of this concept.

KNEE MRI: PATHOLOGY AND PITFALLS IN INTERPRETATION

MENISCAL PATHOLOGY

The Discoid Meniscus

Although the theory has been challenged, the discoid meniscus is generally regarded as a congenital anomaly. This anomaly is more frequent in the lateral meniscus and is usually bilateral.[24] A discoid medial meniscus is a much less common occurrence.

Lateral discoid menisci have been classified as three different types: (1) a complete type, which is

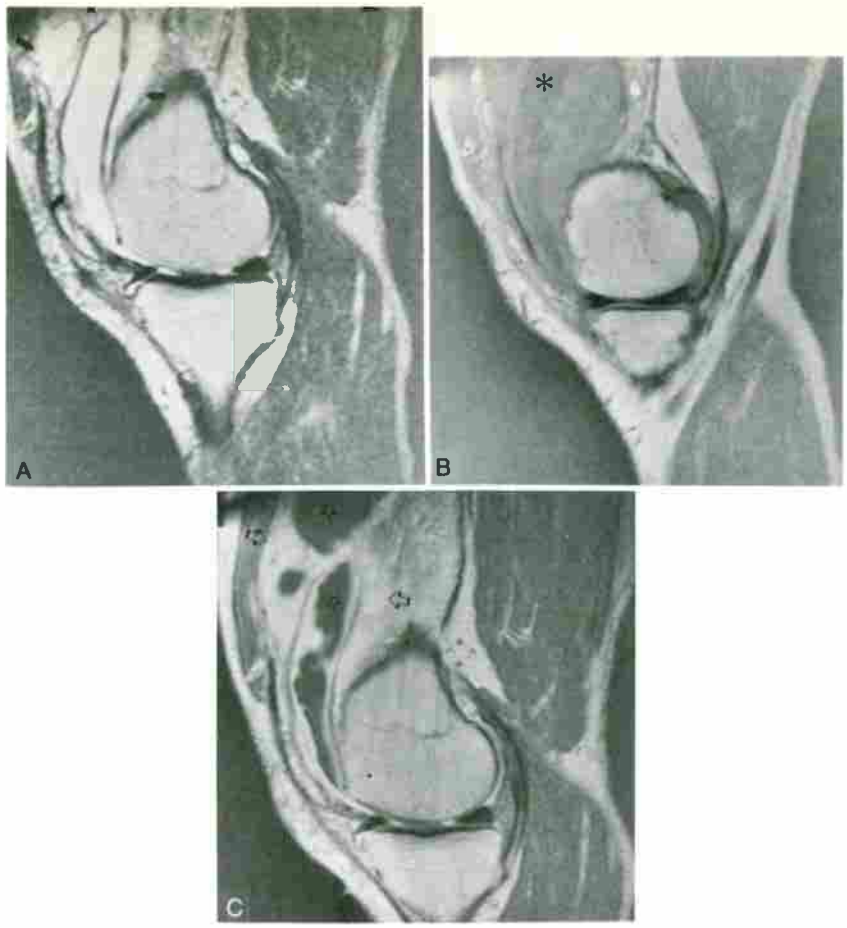

FIG 46. Inflammatory arthritis. **A,** Sagittal T2-weighted (TR/TE, 2000/70) image demonstrates diffuse homogeneous high signal intensity in a distended suprapatellar pouch (arrows). **B,** Sagittal T1-weighted (TR/TE, 717/20) image shows intermediate signal intensity (white arrows) surrounding lower signal intensity (asterisk) in the same region. **C,** Sagittal T1-weighted image after intravenous gadolinium demonstrates peripheral enhancement of the inflamed synovium (open arrows) with the center remaining low signal intensity (stars) because it represents joint effusion. Although the conspicuity of the inflamed synovium is increased after gadolinium injection, note that on the preinjection T1-weighted image **(B),** the synovium and joint effusion show subtle differences in signal intensity.

a full disk that covers the entire tibial plateau and has normal capsular attachments; (2) an incomplete type, which is larger than a normal meniscus and also has normal capsular attachments; and (3) a Wrisberg ligament type, which lacks a posterior capsular attachment except for its attachment to the meniscofemoral ligament. This classification is widely accepted and forms the basis of surgical management.[25-27]

The first two types are usually asymptomatic unless associated with a tear and usually are discovered in adults. The third type, owing to its hypermobility, is associated with the snapping-knee syndrome and usually occurs in children and adolescents. Discoid menisci have an increased incidence of radial or longitudinal tears.[28]

At MRI, the discoid meniscus appears larger than normal. On sagittal cuts, the meniscal bow-tie is identified on more than two consecutive images. The central portion of the bow-tie, representing the body of the meniscus, is thicker and does not taper normally, indicating an abnormally large mediolateral dimension of the body (Fig. 8). The diagnosis of discoid meniscus should be confirmed on coronal images. At the level of the midportion of the knee, the abnormally large meniscus is seen to extend to the intercondylar notch, with an abnormal almost rectangular shape instead of its normal triangular configuration. At times it may be difficult to recognize a discoid meniscus when its configuration is altered by the presence of tears.

Meniscal Tears

Meniscal tears can be classified in two broad categories on the basis of their pathogenesis. A meniscal tear may occur in a traumatic setting when an abnormal force is applied to a normal meniscus.

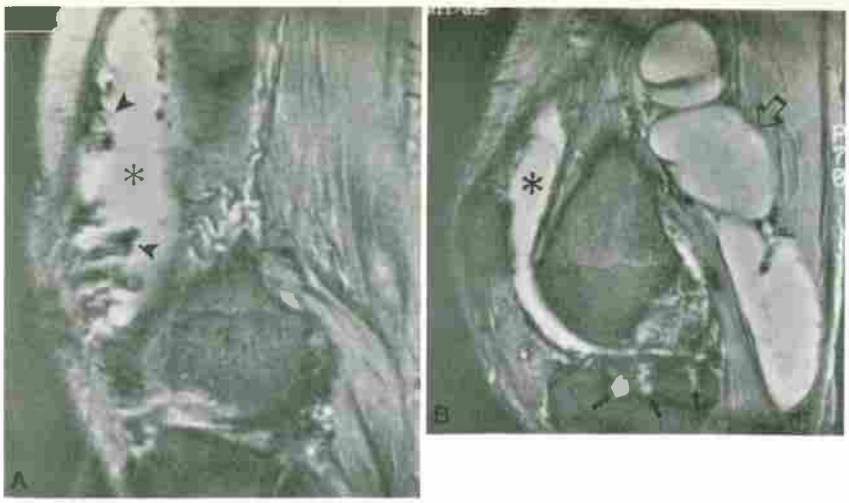

FIG 47. Rheumatoid arthritis. **A, B,** Sagittal gradient-echo (TR/TE, 850/20; angle, 30 degrees) images show a large joint effusion (asterisk). Pannus appears as low-signal-intensity frond-like extensions (arrowheads) contrasting against the high-signal-intensity effusion. The low signal intensity of the synovium indicates chronic synovitis with fibrosis or hemosiderin deposition or both. Large popliteal cyst (open arrow). Subchondral cysts or erosions or both (small arrows).

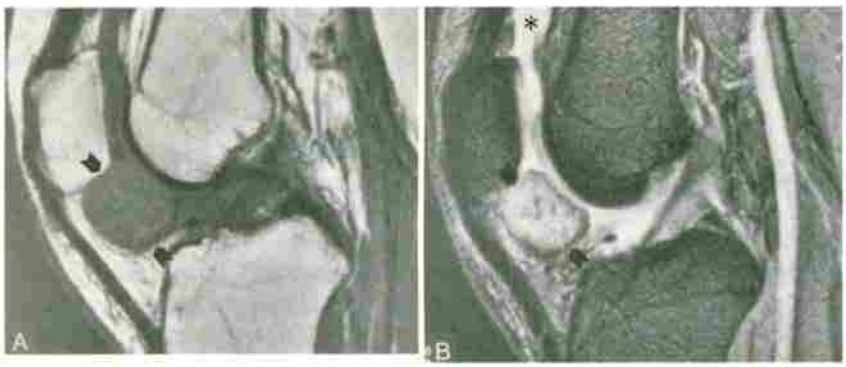

FIG 48. Localized nodular synovitis. **A,** Sagittal T1-weighted (TR/TE, 430/20) image demonstrates an intraarticular, well-circumscribed homogeneous intermediate-signal-intensity mass (arrows) compressing the infrapatellar fat pad. **B,** Sagittal gradient-echo (TR/TE, 442/18; angle, 30 degrees) image shows increased signal intensity with some focal areas of low signal intensity representing hemosiderin deposition in the lesion. Joint effusion (asterisk).

This usually results in a vertical tear, which may propagate in a longitudinal (bucket-handle tear) or transverse (radial tear) direction. A meniscal tear may also be generated by normal forces acting on a degenerated structure. These degenerative-type tears have a tendency to be horizontal cleavage tears, usually in the posterior horn of the meniscus.[24] In general, tears are more frequent in the medial meniscus. Radial tears have a propensity to occur in the lateral meniscus (Fig. 9).

MRI is very accurate in diagnosing meniscal tears. In 1988, in a study that included 242 patients, Mink et al.[29] demonstrated an overall accuracy of 93% in the diagnosis of meniscal tears.

The ultimate criterion for diagnosing a meniscal tear at MRI is the identification of intrameniscal high signal extending unequivocally to at least one meniscal articular surface. If the signal can be seen on more than one MR image, the diagnostic confidence is increased.[30] If the intrameniscal signal does not unequivocally extend to the surface, a meniscal tear is unlikely.[30,31] Abnormal meniscal signal is best depicted on T1W and T2* sequences. The T2W spin-echo images often do not demonstrate an abnormal meniscal signal that is clearly evident on other pulse sequences; this should not dissuade one from making the proper diagnosis of a tear.[16]

A bucket-handle tear results from the longitudinal extension of a vertical tear, usually originating in the posterior horn of the meniscus. As previously mentioned, it usually occurs in a traumatic setting and is seen most frequently in young adults. Although the degree of longitudinal extension of the

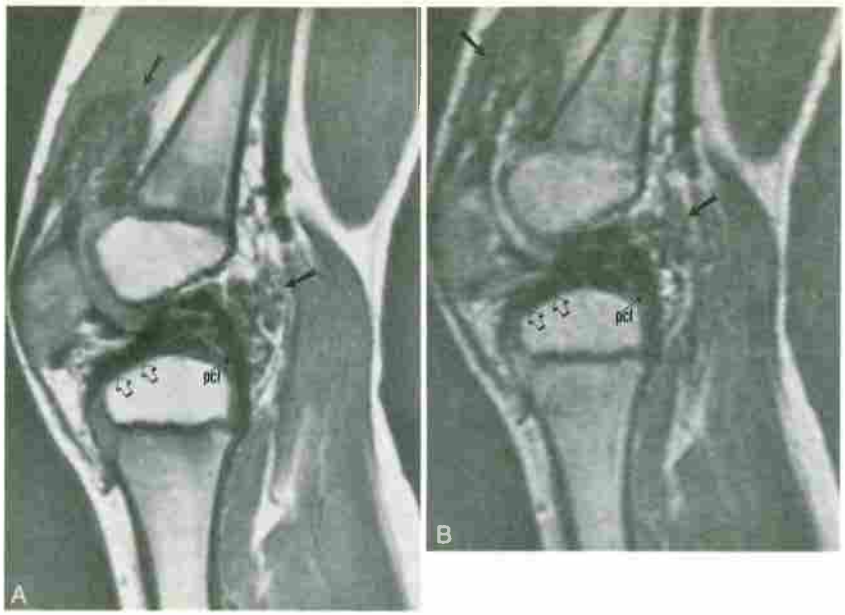

FIG 49. Hemophilic arthropathy. Five-year-old patient with known hemophilia and a swollen right knee. **A,** T1-weighted (TR/TE, 600/25) and **(B)** corresponding T2-weighted (TR/TE, 2000/80) sagittal images demonstrate low-signal-intensity pannus (arrows) in suprapatellar pouch and surrounding the posterior cruciate ligament (pcl). The low signal intensity of the pannus is a reflection of the hemosiderin content. Note that the pannus has eroded the tibial cartilage anteriorly (open arrows). MR depiction of cartilage destruction eliminates synovectomy as a therapeutic option for this patient.

tear toward the anterior meniscal horn may be variable, if extensive, it may allow displacement of the inner fragment into the intercondylar notch. The degree of displacement of the inner fragment is also variable; hence a bucket-handle tear may be displaced or nondisplaced; displaced bucket-handle tears do not necessarily manifest as high signal intensity in the abnormal meniscus. Bucket-handle tears are more frequent in the medial meniscus.

The signs of a bucket-handle tear at MRI relate to the peripheral (bucket) and displaced inner fragment (handle). The longitudinal tear causes shortening of the mediolateral dimension of the body of the meniscus, and on consecutive sagittal images, fewer than two bow-ties are seen. The inner fragment can be displaced for a variable distance over the tibial plateau surface. If displaced as far as the intercondylar notch, in the case of the medial meniscus, the inner fragment can come to lie between the PCL and the underlying tibia. On sagittal views, the fragment appears as a low-signal-intensity longitudinally oriented band lying beneath and parallel to the PCL, creating a double cruciate configuration, referred to as the double PCL sign.[32] On coronal views, the displaced fragment appears as a low-signal-intensity structure located beneath the PCL seen in cross-section. The remaining peripheral portion of the meniscus appears small and has an abnormal configuration (Fig. 10).

Meniscal tears may be horizontal (Fig. 11) or complex (Fig. 12) in their orientation. A complex tear shows high signal extending to the meniscal articular surfaces in more than one direction.

In addition to a high signal intensity extending to the articular surface, a meniscal tear may also be diagnosed on the basis of abnormal size or shape of a meniscus.[33] This usually represents tears of the free edge of the meniscus or truncation of the posterior or anterior meniscal horns.

Meniscocapsular injuries may be seen as a vertical tear involving the most peripheral portion of the meniscus or as a separation between the capsule and the meniscus (Fig. 13). The presence of fluid dissecting between the capsule and meniscus is diagnostic of a meniscocapsular separation and is best appreciated on coronal T2W or T2* images.[34]

Pitfalls in Interpretation of Meniscal Tears

Several potential pitfalls in the evaluation of menisci may confound the inexperienced reader. Wrisberg and Humphry ligaments (Fig. 14) with their surrounding high-signal-intensity loose connective tissue may mimic a tear of the most medial part of the posterior horn of the lateral meniscus.[35, 36] One clue in making the correct diagnosis is to recognize the continuity of the ligaments on successive sagittal images (Fig. 15). In a similar fashion, the transverse meniscal ligament (Fig. 16) can be mistaken for a tear of the anterior horn of the lateral or, less commonly, the medial meniscus (Fig.

17). Again, identifying the ligament on successive contiguous sagittal cuts prevents the diagnostic error.

The popliteus tendon within its synovial sheath is another potential pitfall in interpretation (Fig. 18). Although it separates the lateral meniscus from the joint capsule, the high signal intensity of its synovial sheath or surrounding fluid should not be misinterpreted as a tear of the posterior horn of the lateral meniscus, either on sagittal or coronal images.[37] The key for making the correct diagnosis lies in a thorough knowledge of the anatomy.

On coronal images, the "C" configuration of the posterior horn of the meniscus can simulate a bucket-handle tear, with the inner fragment displaced toward the intercondylar notch (Fig. 19).

Another parameniscal structure that can mimic a peripheral tear of the anterior horn of the lateral meniscus is the lateral inferior geniculate artery, which runs deep to the LCL and appears as a low-signal-intensity structure separate from the margin of the lateral meniscus.[38]

Meniscal Degeneration

A classification for meniscal signal abnormalities was first introduced by Lotysch et al. in 1986.[39] The classification comprises four stages, ranging from a normal, homogeneous low-signal-intensity meniscus (grade 0) to a meniscal tear (grade 3 signal), described as a high or intermediate signal intensity extending to at least one articular surface. Stages 1 and 2, respectively corresponding to globular and linear intrameniscal signal not communicating with any articular surface, were shown to represent myxoid degeneration on histologic examination[40] (Fig. 20).

Intrameniscal degeneration is asymptomatic. Degenerative changes of the meniscus are most frequently observed in the posterior horn of the medial meniscus and become evident on MRI around the age of 30 years, usually as small punctate or linear intrameniscal signals.[41] Later on, around 40 years, the changes become more confluent and may show a triangular configuration. These changes reflect a natural degenerative meniscal process, occur both in men and women, and are independent of level of physical activity. Large areas of myxoid degeneration may predispose to meniscal tear.[42]

Intrameniscal degenerative changes are not visible at arthroscopy and do not affect treatment or outcome. Although different forms of meniscal abnormalities may be visualized at MRI, it is only the diagnosis or exclusion of meniscal tears that is clinically relevant and, as such, should be emphasized in the radiology report.

Meniscal Cysts

Meniscal cysts are always associated with a horizontal meniscal tear and are most frequently associated with the anterior horn of the lateral meniscus (Fig. 21). Synovial fluid from the knee joint is forced through the meniscal tear and accumulates at the meniscocapsular junction. Part of the fluid is resorbed, leaving behind a cystic structure filled with a gelatinous substance.[16] A meniscal cyst can be confined to the meniscal structure or eventually extend into the parameniscal soft tissues (parameniscal cyst). Because of the tight ligamentous anatomy on the lateral side of the knee, lateral parameniscal cysts tend to be small. On the medial aspect of the knee, the ligamentous support being less restrictive, the medial parameniscal cysts can dissect through the joint capsule and become quite large, especially if they occur posterior to the MCL.

Postsurgical Meniscus

After partial meniscectomy, the MRI appearance of the meniscal remnant is variable. Always smaller in size, the residual meniscus may retain a normal triangular shape or have a blunted free edge. In addition, a wide range of MRI configurations, ranging from homogeneous signal with well-defined contour to signal inhomogeneity and marked surface irregularity, have been described as normal postoperative findings.[43]

Tears occurring in the peripheral vascularized portion of the meniscus have the potential to heal with conservative treatment or surgical repair. The healing process involves proliferation of capillaries, formation of fibrous tissue, and ultimately, metaplasia to fibrocartilage-like tissue, which is histologically different from native fibrocartilage.[44] Either spontaneously or surgically repaired, a healed tear will be seen at MRI as a persistent high signal intensity extending to the meniscal surface; caution should be exercised in diagnosing a recurrent or persistent tear in a postoperative meniscus.[44, 45] MRI has been found unreliable in detecting recurrent tears in surgically repaired menisci, especially when there has been extensive resection.[43-47] Recently, a study suggested that MR arthrography is more accurate than conventional MRI at detecting recurrent tears in postsurgical menisci and could be a valuable alternative to arthroscopy in those patients.[48] Further studies are needed to clarify the role of knee MRI arthrography.

INJURY TO THE CRUCIATE LIGAMENTS

Anterior Cruciate Ligament Tears

The ACL is the most frequently torn ligament in the knee.The single most sensitive and specific MRI

sign in the diagnosis of ACL tears is the inability to visualize a normal ACL.[49] The ACL is best imaged in the sagittal plane. Consequently, a major pitfall in interpretation is an inadequate imaging technique, rendering suboptimal sagittal images for the evaluation of the ACL. With adequate imaging technique, MRI is very valuable in diagnosing complete ACL tears with a reported accuracy of 95%[33] and specificity of 100%.[50]

Primary and secondary signs in the diagnosis of complete ACL tears have been described.[49, 51-58] Primary signs are specific signs related directly to the ACL anatomy and consist of (1) focal or diffuse increased signal intensity within the ligament, (2) discontinuity of the ligamentous fibers, (3) abnormal orientation of the ligament in the intercondylar notch, (4) abnormal wavy anterior contour of the ligament, and most important, (5) nonvisualization of the ACL.

Complete ACL tears most frequently occur in the midsubstance of the ligament or at the femoral attachment and only rarely involve the tibial attachment. Complete ACL tears are commonly associated with other knee injuries. In patients with ACL injuries, two recent series reported an associated meniscal tear, of either medial or lateral meniscus, in 68% of the cases, whereas a MCL injury was present in 18% to 24%.[50,57] The well-known terrible triad of O'Donoghue, consisting of the association of acute ACL, MCL, and medial meniscal tears has recently been challenged.[59] In a retrospective study of 60 patients with arthroscopically proven combined ACL–MCL tears, the authors found a statistically significant greater number of associated lateral meniscal tears and stated that the triad of ACL–MCL–lateral meniscal injury is in fact more common than the classic O'Donoghue triad.

Secondary signs of complete ACL tears may be classified into two broad categories: (1) bone marrow abnormalities associated with characteristic injury patterns, and (2) signs of anterolateral instability of the knee resulting from the ACL incompetence.

The ACL is most frequently torn when a valgus stress is applied on an almost fully extended knee. As the ACL ruptures, the tibia subluxes anteriorly and rotates internally relative to the femur. If sufficient force is present, the posterior aspect of the lateral tibial plateau and the middle or anterior surface of the lateral femoral condyle are forcefully impacted on one another, resulting in subchondral occult fractures, referred to as bone contusions[58] (Fig. 22). The presence of bone contusions is a highly reliable sign of a complete ACL tear at MRI.[54] The most frequent pattern is the association of an occult fracture of the posterior aspect of the lateral tibial plateau and of the lateral femoral condyle just above the anterior horn of the lateral meniscus, referred to as "kissing contusions." The next most common pattern is an isolated bone contusion of the posterior aspect of the lateral tibial plateau.

Hyperextension of the knee may cause rupture of the ACL. With this mechanism of injury, the ACL is frequently the only internal structure involved but is commonly associated with bone contusions of the anterior aspect of the femoral condyles and anterior tibia.[53] Finally, a combination of varus stress and internal rotation applied to the knee, causing injury to the lateral collateral complex and an avulsion fracture of the lateral tibial rim (Segond fracture), has a high predictive value for ACL injury.[60] It is also associated with a high incidence of meniscal tears. The Segond fracture may be identified on conventional radiographs as a small cortical avulsion off the middle portion of the lateral tibial plateau just distal to the joint line or be seen at MRI as a bone contusion of the lateral tibial rim. Either of these findings should prompt the search for associated meniscoligamentous injury.

ACL rupture results in anterolateral instability of the knee and allows anterior translation of the tibia relative to the femur. Two secondary signs of ACL tears are a consequence of this instability: (1) buckling of the PCL and (2) posterior displacement of the posterior horn of the lateral meniscus relative to the lateral tibial plateau (uncovered lateral meniscus).[48, 53, 55] Other studies have measured the degree of anterior tibial subluxation.[55, 56]

In addition to the secondary signs and evaluation of the ACL on sagittal images, examination of the ACL both on coronal and axial images may aid in the diagnosis of a complete ACL tear. Inability to identify a normal ACL in the lateral aspect of the intercondylar notch on coronal images, or the presence of a mass effect of low signal intensity on T1W images and high signal intensity on T2W or gradient-echo images, representing edema and hemorrhage, in the expected location of the ACL, is a sign consistent with an ACL tear. Similarly, nonvisualization of a normal ACL on axial images may increase diagnostic confidence of an ACL tear.

A well-recognized pitfall in ACL tear is the pseudomass at the proximal portion of the ACL, resulting from partial volume averaging of the lateral femoral condyle. If the distal and middle segments of the ligament appear intact, the ACL will usually be normal even if its proximal aspect is not well visualized. A cadaveric study has also demonstrated the presence of mucoid or eosinophilic degeneration within the ligament, which may be seen as focal high signal on MRI and potentially mimic a tear.[61] These focal areas of degeneration are simi-

lar to those encountered in the menisci. They are more likely to occur in older individuals. Hence, focal high signal intensity in an ACL with intact margins and normal course may be a manifestation of the normal aging process.

Differentiation of partial from complete ACL tears at MRI is difficult but is important because patients with incompletely torn ACL will preferably be treated conservatively. Partial ACL tears may be seen with intrasubstance edema and hemorrhage, depicted at MRI as focal low to intermediate signal on T1W sequences and relatively high signal on T2W or T2* images. Alternatively, the ligament may show signs of laxity on MRI, with an inferiorly bowing or sagging contour. The absence of secondary signs of complete ACL tear may also help rule in favor of partial ligamentous disruption.

The hallmark of a chronic tear of the ACL is the absence of edema associated with nonvisualization of the ACL or identification of ligamentous disruption.[62] Scar tissue in the intercondylar notch can occasionally create a confusing appearance in chronic ACL tears. The low-signal-intensity fibrous scar runs along the expected course of the ACL and can be mistaken for an intact ligament. Another situation that may be mistakenly diagnosed as normal occurs when the ACL ruptures proximally, and the torn fragments scar down to the lateral aspect of the PCL close to the normal femoral insertion site of the ACL (Fig. 23). This creates a low-signal-intensity straight band with the orientation of a normal ACL and may be difficult or impossible to distinguish from an intact ligament. Any angulation of the ACL should alert one that there may be a chronic ACL tear with scarring.[16]

Postoperative ACL Reconstruction

Reconstructive surgery of the ACL is a widely accepted and frequently performed technique used to restore anterolateral stability to the knee, usually in young individuals or athletes. There are different types of reconstructions, some using autogenous semitendinosus, gracilis, or iliotibial tract tendons, and others using part of the patient's patellar tendon combined with a small attached fragment of bone on each end of the graft from the patella and tibial tuberosity. The graft material may also be synthetic or cadaveric. The graft is inserted through drilled tunnels in the proximal tibia and lateral aspect of the intercondylar roof, ideally recreating the anatomy of the native ligament.

MRI provides excellent visualization of an intact reconstructed ACL.[63-65] The appearance of the ACL graft is similar to that of a native ligament, and the same diagnostic criteria can generally be applied to assess its integrity (Fig. 24). Much of the success of the surgery depends on optimal placement of the ACL graft. If the tibial tunnel is placed too far anteriorly, the reconstructed ACL is impinged on by the roof of the intercondylar notch and may be forced to angulate about its distal edge. Impingement may also be caused by osteophytes arising from the intercondylar roof. Consequently, the ACL graft is subjected to repeated deleterious strain each time the knee is extended and may be weakened and ultimately may rupture. A normal unimpinged reconstructed ACL appears as a homogeneous low-signal band on MRI. A graft with impingement shows increased signal intensity, mainly in the distal two thirds of the ligament, and is associated clinically with a greater incidence of instability and persistent flexion contractures.[66, 67]

Posterior Cruciate Ligament Tears

Although PCL tears are a much less frequent occurrence than ACL injuries, the recent trend toward surgical repair of acute PCL tears emphasizes the need for their early diagnosis. The PCL is the largest ligament of the knee and is consistently and easily visualized at MRI without being affected by minor degrees of knee rotation. The reported accuracy of MRI in diagnosing PCL complete tears is 100%.[68] Rupture of the PCL usually implies severe trauma to the knee and is frequently associated with other meniscoligamentous injuries to the knee.[69]

Complete tears of the PCL most commonly occur within the midsubstance of the ligament (Fig. 25). PCL insufficiency may also result from avulsion of the tibial insertion with or without an attached bony fragment (Fig. 26). The most frequent mechanisms of PCL injury are (1) a direct blow to the anterior aspect of the tibia resulting in sudden forceful posterior translation of the tibia, and (2) forced hyperextension of the knee. In these circumstances, a PCL tear may be associated with bone contusions or fractures of the anterior proximal tibia and lateral femoral condyle, as well as with other meniscoligamentous injuries.[70]

A complete PCL tear may be identified at MRI as (1) inability to visualize the ligament, (2) nonvisualization of the ligamentous fibers with diffuse areas of high signal intensity on T1W and T2W or T2* images in the expected course of the ligament, and (3) identification of the ligamentous fibers with focal complete interruption.

A partially torn PCL may show thickening with intrasubstance of edema and hemorrhage with some of the ligamentous fibers remaining intact. Chronic tears may heal by a low-signal-intensity scar that resembles an intact, normal ligament. Chronic tears may also demonstrate persistent

streaks of high signal intensity within a ligament with intact margins.[16]

INJURY TO THE COLLATERAL LIGAMENTS

Medial and Lateral Collateral Ligament Tears

Injuries to the MCL and LCL, respectively, result when valgus and varus forces are applied to the knee. These injuries may be isolated or occur as part of a more extensive meniscoligamentous trauma.

A partially torn (or sprained) MCL may be seen with thickening of the ligament with intrasubstance focal or diffuse high signal intensity, representing edema or hemorrhage or both, but the continuity of the ligament is maintained (Fig. 27). Fluid can also be identified in the surrounding soft tissues, which may be the first finding to draw attention to a possible MCL injury. Complete tears of the MCL are diagnosed when complete interruption of the ligamentous fibers is identified (Fig. 28). The remaining ligament may have a wavy appearance because it is no longer held taut between its tibial and femoral insertions. Bone contusions affecting the lateral side of the joint may be associated, reflecting the valgus mechanism of injury.[71]

A recent retrospective study of 23 surgically proven MCL tears found that although MRI is sensitive in identifying MCL injuries, the severity of the tears was frequently underestimated at MRI examination and suggested that using coronal T2W or T2* pulse sequences could help increase MRI accuracy.[72]

Posttraumatic ossification or calcification either at the insertion site or within the substance of the MCL (Pelligrini–Stieda syndrome) is a reflection of chronic ligamentous injury.[73] At MRI, it may be identified as a focal area of low signal intensity.

Lateral collateral ligament injury diagnosed at MRI consists mainly of complete tears (Fig. 29). LCL injuries are far less common than those of the MCL. High signal intensity extending through the entire width of the disrupted ligament, associated with a wavy contour of the ligament remnants, is the rule.

INJURY TO THE QUADRICEPS AND PATELLAR TENDONS

Quadriceps Tendon

Partial or complete tears of the quadriceps tendon are relatively uncommon injuries and usually occur in individuals older than 40 years. They may be posttraumatic, but most occur in a tendon weakened by infection, inflammation, or mucoid degeneration. Recognized risk factors that weaken tendons are diabetes, chronic renal insufficiency patients on dialysis, oral administration or local injection of steroids, rheumatoid arthritis, gout, and systemic lupus erythematosus.

Complete rupture of the quadriceps tendon may sometimes be mistaken for a neuropathy because of weakness, but in most cases, is accurately diagnosed clinically on the basis of loss of extensor function, the presence of a palpable mass or depression above the patella, or the presence of a hemarthrosis. The role of MRI is to confirm the diagnosis and help plan surgical repair by demonstrating the location, extension, and morphology of the tear, separation of fragments, and quality of the tendon remnants. A complete rupture of the quadriceps tendon is seen as discontinuity of the tendon fibers. If the tear communicates with the suprapatellar pouch, a large hemarthrosis may be present.

Partial quadriceps tendon tears are more frequent and more difficult to evaluate on physical examination. MRI of partial quadriceps tendon tears shows a focally thickened tendon with abnormal increased signal intensity, usually near the superior pole of the patella. Partial ruptures may also be seen as focal interruption of specific tendon layers with the other layers still intact[23] (Fig. 30). A corrugated appearance of the patellar tendon may be an indirect sign of quadriceps tendon injury and demands careful examination of the extensor mechanism.[74]

Patellar Tendon

Patellar tendon injuries are usually seen in individuals younger than 40 years. Complete patellar tendon rupture may result from an acute traumatic injury and most commonly occurs near the inferior pole of the patella or at the tibial insertion. Discontinuity of the tendon is seen at MRI (Fig. 31). These generally occur in regions of the tendon weakened by preexisting partial tears or degeneration.

Jumper's knee, also referred to as patellar tendinitis or partial patellar tendon tear, is seen in young individuals involved in activities in which the extensor mechanism of the knee is put under significant stress by repetitive actions of acceleration, deceleration, jumping, and landing.[75] Histologic examination of the tendon has demonstrated areas of partial tearing of the patellar tendon fibers combined with myxoid degeneration and necrosis, as well as regeneration with fibroblast proliferation. These changes are most frequently seen in the proximal patellar tendon, but the distal quadriceps tendon and the patellar tendon near its tibial insertion may also be affected. MRI demonstrates focal thickening of the tendon, usually associated with increased abnormal signal intensity (Fig. 32).

Patients demonstrate chronic pain in the region of the patellar or quadriceps tendon before, during, or after exercise. If left untreated, this may generate a complete tear of the affected tendon. This is one of the many abnormalities that may cause anterior knee pain, and MRI can help distinguish the etiology of such pain.

In skeletally immature adolescents and preadolescents, the tension on the extensor mechanism is concentrated at the growth plates and may lead to tendinitis of the distal patellar tendon and sometimes to cartilaginous or osseous avulsion of the tibial tuberosity (Osgood–Schlatter disease). In a recent study of 28 cases of Osgood–Schlatter lesion, Rosenberg et al.[76] demonstrated a 100% prevalence of soft-tissue abnormalities and 37% prevalence of bony pathology in their patients. At MRI, soft-tissue changes consisted of thickening and increased signal intensity of the tendon at the tibial insertion, and deep or superficial infrapatellar bursitis was also commonly seen. The presence of a small ossicle anterior to the ossification center of the tibial tuberosity and changes in marrow signal in the tibial tuberosity and tibial epiphysis thought to represent marrow edema constituted the bony abnormalities.

Sinding–Larsen–Johansson disease similarly is a traction epiphysitis occurring at the inferior pole of the patella and may lead to fragmentation of the secondary ossification center.

PATELLOFEMORAL JOINT

The patellofemoral joint is a frequent source of knee pain. The symptoms are not always specific, and patients may have a clinical presentation that mimics other forms of internal derangements of the knee. Common pathology of the patellofemoral joint includes patella fracture, dislocation, and chondromalacia, as well as patellar alignment and tracking abnormalities.

Patellar Alignment and Tracking

During flexion of the knee, the patella migrates downward in a vertical plane and is normally centered in the femoral trochlear groove during the entire excursion. Although arthroscopy is still considered the gold standard for evaluation of patellar tracking abnormalities, many authors have described their experience with a kinematic MRI technique and have shown promising results with this noninvasive technique.[77-79]

Patellar alignment relates to the relationship between the patella and femoral trochlear groove when the knee is extended.[80] Several methods of evaluation of patellar alignment on cross-sectional imaging have been described, and recent reports have shown high correlation between abnormal patellar tracking and the position of the patella in the extended knee.[78] A frequently used measurement is the patellar tilt angle formed by a line tangent to the lateral facet of the patella and a second line parallel to the posterior aspects of the medial and lateral femoral condyles. The normal angle is greater than 8 degrees. Other measurements (congruence angle, lateral patellar displacement) evaluate lateralization of the patella. These measurements can be performed on MR axial images with the knee in 5 degrees of flexion (some investigators believe that a slight degree of patellar tilt is a normal finding when the knee is fully extended[81]) and alert to potential abnormality of the patellar tracking mechanism. In addition, morphological abnormalities such as patella alta, misshapen patella, and abnormal configuration of the femoral trochlear groove may be identified on MR examination and can also be a sign of patellar tracking abnormality (Fig. 33).

Dislocation of the Patella

Dislocation of the patella often is not suspected at clinical examination of an acutely injured knee. In most cases, the patella has spontaneously relocated in the femoral trochlear groove before physical examination, and a clear history of the exact mechanism of injury is only rarely elicited. Presumptive diagnosis of a prior transient patellar dislocation may first be suggested at MRI.

In a traumatic setting, lateral dislocation of the patella usually results from internal rotation of the femur on a fixed tibia, associated with forceful contraction of the quadriceps muscle. As the patella dislocates or when it spontaneously relocates, the medial facet of the patella impacts against the lateral femoral condyle. In addition, lateral displacement of the patella strains significantly the medial retinaculum and the medial aspect of the joint capsule.

The findings at MRI reflect the mechanism of injury (Fig. 34). The medial retinaculum may remain intact. In other instances, it may be stretched and have a wavy contour, be thickened, or be partially or completely torn, showing, respectively, partial disruption or discontinuity of the low-signal-intensity thin band. Associated edema in the adjacent soft tissues may be seen in all instances. The medial retinaculum may also be avulsed from its patellar insertion. Bone contusions and chondral or osteochondral fractures may occur at the anterolateral aspect of the lateral femoral condyle or on the medial facet of the patella. The combination of both findings may also occur. Bone contusions appear as geographic low-signal-intensity lesions on

T1W images, show increased signal intensity on T2W sequences, and involve the cancellous bone. Chondral or osteochondral fractures are seen as chondral or bony defects, respectively, and may lead to the formation of loose bodies. In three recent studies, osseous abnormalities were most frequently seen in the lateral femoral condyle and are thought to represent a highly specific sign of patellar dislocation.[82-84] Finally, a hemarthrosis is also frequently seen in the acute dislocation of the patella.

BONE MARROW DISORDERS

Hematopoietic Hyperplasia

At birth, the entire skeleton is composed of hematopoietic (red) marrow. In the first few months of life, conversion to fatty (yellow) marrow occurs in the epiphyses of long bones. Progressively, during childhood and adolescence, conversion to fatty marrow in the appendicular skeleton proceeds in a sequential manner. The process starts in the diaphysis and progresses to the distal metaphysis and finally to the proximal metaphysis. By young adulthood, usually around 25 years of age, hematopoietic marrow is confined to the axial skeleton, proximal humeri, and femora. Under certain conditions, fatty marrow may undergo reconversion to hematopoietic marrow, with hyperplasia of residual hematopoietic cells. This fatty marrow reconversion begins in the proximal metaphysis and then involves the distal metaphysis and finally the diaphysis of long bones, the reverse of the original physiologic process.[85] The proximal bones of the appendicular skeleton undergo reconversion to red marrow before the more distal bones.

Hematopoietic marrow is intermediate to low signal intensity on T1W sequences and remains of intermediate signal intensity or shows slight increase in signal intensity on T2W sequences. On routine imaging of the knee, hematopoietic marrow is best evaluated on T1W sequences, in which the contrast between hematopoietic and fatty marrow is maximized.

Small foci of metaphyseal red marrow interspersed between fatty marrow are often identified in the distal femur, on knee MRI studies in patients older than 25 years, and are of no clinical significance.[86] More diffuse, homogeneous hematopoietic hyperplasia seen as metaphyseal confluent areas of intermediate to low signal intensity on T1W images may be observed in chronic anemias, benign and malignant infiltrative marrow disorders such as Gaucher's disease, myelofibrosis, myeloma, and metastatic disease, as well as heart disease with chronic heart failure.

Some investigators have described red marrow expansion in mildly to moderately obese women who were otherwise healthy[87] (Fig. 35). Discovered as an incidental finding on routine knee MRI studies, this process is not fully understood but is believed to be benign. Nevertheless, peripheral blood analysis may be valuable to rule out any marrow disorder in these patients. Hematopoietic hyperplasia has also been described as a normal finding in marathon runners and is believed to be the result of "sports anemia" often seen in high-level athletes involved in aerobic sports.[88] Finally, similar findings have been observed in smokers and are believed to be related to increased oxygen requirements.

Interestingly, fatty marrow reconversion in the proximal tibial metaphysis is much less frequently seen than in the distal femoral metaphysis as an incidental finding in healthy subjects. Because reconversion occurs in a proximal-to-distal fashion, the presence of red marrow expansion in the proximal tibia may be a sign of a more extensive process and raises the possibility of an underlying disease.[86] Red marrow should not be seen in the epiphysis except in the infant. The presence of low signal intensity in the epiphysis on T1W sequences should prompt an investigation to rule out neoplastic processes such as leukemia, lymphoma, or metastases.

Medullary Infarcts

There are many well-recognized etiologies of bone medullary infarcts, and the most frequent causes are idiopathic, alcoholism, corticosteroid therapy, systemic lupus erythematosus and other vasculitides, sickle cell disease, Gaucher's disease, pancreatitis, and radiotherapy.

On plain films, bone infarctions have a characteristic appearance and appear as serpiginous, shell-like calcifications usually in the metadiaphysis of long bones, but they also often involve the epiphyseal regions. Their appearance is similar on MRI. They are seen as serpiginous lesions with low-signal-intensity borders with the center remaining intermediate to high signal intensity on T1W and T2W sequences, but they are best depicted on T1W sequences (Fig. 36). In the acute stage, there may be some increased signal intensity within the lesion on T2W or T2* images, thought to represent edema. The low-signal-intensity contours of the lesion correspond to the calcific density seen on plain films. Immature infarcts that are not visible on plain films because of the absence of calcification may be detected on MRI. In these circumstances, the low-signal-intensity borders are thought to represent fibrotic tissue at the interface between necrotic and

viable bone.[86] MRI is also more specific than radionuclide imaging for the diagnosis of bone infarcts.

Spontaneous Osteonecrosis of the Knee

Spontaneous osteonecrosis of the knee is seen in middle-aged and elderly patients, usually women, and is seen as sudden onset of acute, localized pain to the knee. It most frequently occurs in the medial femoral condyle, typically involving the weight-bearing surface. Other sites of involvement in decreasing order of frequency are medial tibial plateau, lateral femoral condyle, and lateral tibial plateau. Its exact cause is still unclear, but it could be secondary to repeated microtrauma, ultimately resulting in ischemic necrosis. An association between meniscal tears and spontaneous osteonecrosis of the knee has been established, and some investigators have suggested that a meniscal injury may be the first event preceding the development of osteonecrosis of the knee.[89]

At initial presentation, the plain radiographs are usually normal. MRI can show diagnostic findings in the early stages of osteonecrosis because of its increased sensitivity to bone marrow disorders. The lesion appears as a focal subcortical low signal intensity on T1W images in the femoral condyle or tibial plateau. On T2W sequences, increased signal intensity is seen reflecting the presence of bone marrow edema.

LESIONS OF BONE AND CARTILAGE

Bone Contusions

Bone contusions are occult subcortical fractures thought to represent areas of trabecular microfractures associated with hemorrhage and edema. In a study of patients with posttraumatic hemarthrosis, the prevalence of occult subcortical fractures was 72% .[90] Bone contusions are frequently associated with meniscoligamentous injuries and occur most commonly in the lateral femorotibial compartment. The pattern or precise location of contusions often indicates the mechanism of injury and what associated abnormalities will be present.

Bone contusions are best depicted on T1W sequences, where they appear as areas of reticular or geographic low signal intensity in the subcortical cancellous bone.[91] They may be contiguous with the subjacent cortical bone, but the osteochondral component of the subjacent articular surface remains intact. Bone contusions appear as areas of increased signal intensity on T2W, T2,* and fat-suppression sequences. They will normally resolve in approximately 6 to 8 weeks.

Acute bone contusions are clinically symptomatic. In addition, they can lead to premature degenerative joint disease.[86,90] As healing occurs, the trabeculae become thickened, rendering the subchondral bone less resilient to normal weight-bearing stresses. Consequently, increased forces are transmitted to the articular cartilage and may lead to early degeneration. Bone contusions may heal without sequelae or become areas of chronic low signal intensity on all pulse sequences, presumably representing areas of fibrosis in the subcortical bone. Appropriate treatment with limited weight-bearing is considered necessary in many cases to prevent these contusions from progressing to osteochondral fractures.

Osteochondral Fractures

Impaction fractures result in variable degrees of depression of the osteochondral articular surface and are most often associated with a contiguous geographic bone contusion. The involved cortex is depressed or fractured. At MRI, there may be discrete disruption, irregularity, or depression of the thin low-signal cortical line at the impaction site, on all pulse sequences. Thinning of the overlying intermediate-signal-intensity cartilage is best depicted on T2* images.

Osteochondral fractures may also be seen as cortical fractures associated with a subcortical cancellous bone component. The overlying hyaline cartilage is intact. The osteochondral fracture fragment may remain in situ or become detached from the host bone. In the former, the interface with the donor site is demarcated by a low-signal-intensity rim on T1W images and intermediate, inhomogeneous signal intensity on T2W or T2* images. In the latter instance, the interface shows high signal intensity on T2W or T2* images, representing joint fluid infiltrating between the donor site and the osteochondral fragment. A detached osteochondral fragment may eventually become a loose body. Osteochondral fractures may lead to premature degenerative joint disease.

Stress Fractures

MRI is a sensitive imaging technique for the early diagnosis of stress fractures and, in most instances, is a more specific imaging modality than bone scans.

Stress fractures may be subdivided into two broad categories: fatigue fractures and insufficiency fractures. Fatigue fractures occur in normal bones that are subjected to abnormal stresses and are usually seen in younger individuals. Insufficiency fractures result from normal physiologic stresses applied to abnormal bones (osteoporosis, osteomalacia, radiation therapy, neoplastic diseases, etc.).

They are most frequent in an older population and particularly in women.

Stress fractures occurring in cancellous bone will be seen at MRI as linear or amorphous low-signal-intensity areas on T1W images and may become high signal intensity on T2W sequences (Fig. 37). The linear areas are usually perpendicular to the adjacent cortex. Accompanying bone marrow edema is low signal on T1W and high signal on T2W or fat-suppression sequences. Stress fractures involving predominantly cortical bone are usually seen in the diaphysis of long bones. At MRI, a focal, linear, transversely oriented area of disruption of the low-signal-intensity cortex will be seen, sometimes associated with a periosteal reaction.[92] Adjacent bone marrow edema may also be present.

Tibial Plateau and Femoral Fractures

Occult tibial plateau and femoral fractures can sometimes be discovered at knee MRI, after a traumatic injury. A linear pattern of abnormal signal intensity may extend to the articular surface in the case of a tibial plateau fracture or extend across the supracondylar region in the instance of a distal femoral fracture. A broader, ill-defined component of decreased signal intensity on T1W sequences and showing increased signal intensity on T2* images, thought to represent hemorrhage and edema, accompanies the fracture. Impaction and incongruity at the articular surface may also be seen.

Osteochondritis Dissecans

Osteochondritis dissecans usually has its onset in adolescence, and although its exact pathogenesis is still debated, the most widely accepted theory is that of repeated trauma. The lesion may be asymptomatic or mimic internal derangement of the knee. Osteochondritis dissecans most frequently involves the lateral non-weight-bearing surface of the medial femoral condyle (Fig. 38). The osteochondral fragment may remain in situ, be partially detached, or become a loose body in the joint cavity. The treatment, either surgical or conservative, will be based on the relative stability of the osteochondral fragment. MRI has been found to be a noninvasive, specific, and sensitive technique for differentiating loose from stable fragments.[93] The most reliable sign of loosening at MRI is the presence of fluid between the osteochondral fragment and the host bone. Fluid is seen as linear intermediate signal intensity insinuating at the interface between the osteochondral fragment and the parent bone on T1W images, with increased signal intensity on T2W and T2* sequences. A potential pitfall is that granulation tissue shows similar signal intensities and can also be found at the interface between the parent bone and osteochondral fragment. This dilemma creates a potential indication for intravenous administration of gadolinium or knee MR arthrography to make the differentiation.

Degenerative Joint Disease

Osteoarthritis involves the knee more than any other joint. MRI, with its multiplanar capabilities, is certainly promising as a noninvasive procedure for evaluation of the cartilage; however, despite the many pulse sequences studied, the results have been disappointing, and no consensus has been reached on the best imaging sequences.[94-96] Despite its limitations, a standard knee MR study can serve as a general survey in the assessment of degenerative joint disease.

Hyaline cartilage may show signs of early degeneration as focal low-signal-intensity areas on all pulse sequences. More advanced disease will appear as irregularity, thinning, or complete loss of the articular cartilage. Eburnation of the subchondral bone appears as focal low signal intensity on all pulse sequences. Osteophytes when mature show central fatty marrow lined by a low-signal-intensity cortical line. Subchondral cysts or geodes are seen as low- or intermediate-signal-intensity lesions on T1W and high signal intensity on T2* sequences, usually in close proximity to the joint surface. Finally, MRI may also depict loose bodies in the joint cavity. In general, MR is sensitive to moderate or severe degenerative changes in cartilage and cannot reliably depict mild changes.

CYSTIC MASSES IN AND AROUND THE KNEE

Popliteal Cysts

A popliteal cyst or Baker's cyst is a synovial cyst resulting from a communication between the knee joint and the gastrocnemiosemimembranosus bursa, which is located posterior to the medial femoral condyle between the tendons of the medial head of the gastrocnemius and semimembranosus muscles. Any condition generating a joint effusion can lead to the formation of a popliteal cyst.[97] The incidence increases with age.[98] A popliteal cyst may be seen as an asymptomatic mass in the popliteal fossa or, when it ruptures, gives rise to a symptomatology mimicking thrombophlebitis or acute tear of the plantaris tendon.

MRI is exquisitely sensitive in depicting popliteal cysts. On T2W or T2* sequences, the origin of the cyst between the gastrocnemius and semimembranosus tendons is precisely depicted on axial images as a high-signal-intensity neck connecting the joint and the bursa on the posteromedial aspect of the knee. The enlarged bursa is seen as a well-

circumscribed cystic mass of high signal intensity (Fig. 39). The exact extent of the cyst can be assessed in different planes. On T1W images, a popliteal cyst appears of intermediate signal intensity. If traumatized or hemorrhagic, the cyst may show high signal intensity on T1W images or heterogeneity with areas of low signal intensity from blood-degradation products; the appearance depends on the age of the blood.

Ganglion Cysts

Ganglion cysts are benign lesions that may appear clinically as palpable masses around the knee in atypical locations for popliteal cysts. Oftentimes they are discovered as an incidental finding on a knee MR study performed for other reasons. Their exact pathogenesis is still a controversial subject.[99] Unlike meniscal cysts, ganglion cysts are not associated with a meniscal tear. They may show a communication with the joint cavity but may also occur in remote locations, such as within muscle bundles or in apposition to tendon sheaths.[100] A ganglion cyst adjacent to the tibiofibular joint may appear clinically as a peroneal nerve palsy.

Ganglion cysts appear on MRI as well-circumscribed masses with smooth walls. Internal septations are frequently seen, as is a lobular configuration (Fig. 40). Sometimes pseudopodia are seen extending from the main ganglionic cavity.[101] They are filled with a gelatinous, mucoid component with a variable protein concentration. The signal intensity on T1W sequences ranges from low to intermediate. Intermediate signal intensity on T1W images is seen when there is a high protein content. All ganglion cysts show increased signal intensity on T2W and T2* images.

Ganglion cysts may occur in an intraarticular location and clinically may simulate internal derangement of the knee. Intraarticular ganglions are most often found in relation to the cruciate ligaments[101, 102] (Figs. 41 and 42).

Bursae

As discussed in the normal anatomy section, numerous bursae exist around the knee, and when they become inflamed, they can be seen as cystic masses on MRI. Their signal characteristics are indistinguishable from those of synovial cysts or ganglion cysts, but the knowledge of their typical locations will allow the correct diagnosis (Figs. 43-45).

ARTHRITIC DISORDERS

Inflammatory Arthritis

Rheumatoid arthritis, juvenile rheumatoid arthritis, and the three major spondyloarthropathies (ankylosing spondylitis, Reiter's syndrome, and psoriasis) have in common many pathologic features, including synovial inflammation, pannus formation, destruction of cartilage, and bone erosions. Traditionally, diagnosis has been based on clinical presentation, laboratory data, and conventional radiographs. MRI is another diagnostic tool for the evaluation of synovial inflammation and pannus, bone erosions, and cartilage destruction, and shows promising results in assessment of response to treatment.[99] The practical role of MR for evaluation of arthritis remains uncertain.

Synovitis and pannus, the early stages of an inflammatory arthritis, are not reliably distinguished from joint effusion on either T1W or T2W sequences, because they have similar signal intensities. On careful inspection of T1W images, inflamed synovium can be seen as slightly higher signal intensity than joint fluid.

Different authors have studied the effect of intravenous gadolinium injection and demonstrated that inflamed synovium and pannus showed significant enhancement, permitting easy and reliable differentiation from effusion[104-107] (Fig. 46). On contrast-enhanced T1W images, pannus appears as high-signal synovial thickening with nodular or frond-like projections extending variably over the articular surfaces of the knee joint; joint fluid remains low signal intensity and can be easily distinguished from the synovitis. Sometimes, areas of low signal intensity on T1W and T2W sequences may be seen representing hemosiderin deposits, as inflamed synovium is known for its propensity to bleed (Fig. 47).

MRI is more sensitive than plain film for the detection of bone erosions. These appear as subchondral or marginal defects of low signal intensity on nonenhanced T1W sequences and show increased signal intensity on T2W sequences. Without contrast enhancement, it is impossible to differentiate between fluid and pannus infiltrating the erosions, but after gadolinium injection, again pannus demonstrates enhancement, whereas fluid will remain of low signal intensity on T1W images.

Cartilage destruction, resulting either from the inflammatory process or from secondary degenerative changes, will be seen as diffuse thinning or focal defects.

Pigmented Villonodular Synovitis

Pigmented villonodular synovitis (PVNS) is a vascular proliferative disorder of the synovium of unknown etiology, which most commonly involves the tendon sheaths of the fingers but also can be seen in different joints and bursae.[108] When it involves the joints, it is essentially a monoarticular

process and occurs in order of frequency in the knee, hip, and shoulder. It may appear as a localized, intra- or extraarticular form, or as a diffuse form (Fig. 48).

Histologically, villonodular synovial proliferation is found to be a mixture of fibrous tissue, giant cells, xanthoma cells, lymphocytes, and a variable amount of hemosiderin.[99] MRI is presently the best imaging modality to evaluate PVNS. The MR characteristics of PVNS will depend on the proportion of fibrous tissue, fat, and hemosiderin present. On T1W sequences, the synovial lesions show heterogeneous signal intensities. Some areas become low signal intensity on T2W images and even lower signal intensity on T2* sequences because of the magnetic susceptibility effect of hemosiderin.[109] A joint effusion is often present, as well as bone erosions, which are best delineated with MRI. Diffuse enhancement of the synovium will occur with intravenous gadolinium because of the high vascularity of these lesions. In cases of diffuse involvement, the differential diagnosis should include chronic rheumatoid arthritis and hemophilia. The localized form will have to be differentiated from other tumoral processes of the synovium, namely, synovial hemangioma and synovial sarcoma.[110]

Hemophilia

Hemophilia A and Christmas disease (hemophilia B) are X-linked recessive disorders of blood coagulation manifested clinically in men and are frequently associated with intraosseous and intraarticular bleeding.[111] The most frequently affected joints are the knee, elbow, and ankle, in order of decreasing frequency. Pathologically, repeated episodes of bleeding lead to hypertrophy of the synovium, pannus formation, and hemosiderin deposition. Subsequently, cartilage destruction, bone erosions, and intraosseous bleeding leading to cyst formation occur. MRI is very sensitive in detecting early articular damage and may play an important role in making appropriate therapeutic decisions (Fig. 49).

As seen on plain radiographs, certain morphologic abnormalities, such as ballooning of the femoral epiphysis, enlargement of the intercondylar notch, and squaring of the patella can also be assessed with MRI. In addition, MRI portrays the synovial thickening and pannus as low signal intensity on T1W images and also as low to intermediate signal intensity on T2W sequences, reflecting the hemosiderin content. Areas of high signal intensity on T2W images may also be present, representing joint effusion. Cartilage destruction and bone erosions are best visualized with MRI. A characteristic of hemophilic arthropathy is the presence of subchondral cysts thought to be the result of intraosseous bleeding. One MR study demonstrated that these cysts undergo different stages, from collection of fresh blood, subsequent transformation into old hemorrhage, to the formation of fibrous tissue.[112] These successive stages are characterized at MRI by different signal intensities on T1W and T2W images.

CONCLUSION

Although radiographs remain the initial investigative step in diagnosing abnormalities of the knee, MRI is the imaging modality of choice for the evaluation of intraarticular and periarticular disorders of the knee. Its high negative predictive value and diagnostic accuracy in the diagnosis of internal derangement of the knee have been demonstrated by many authors. Diagnostic accuracy is dependent on image quality and interpretative skills of the radiologist. Obtaining state-of-the-art images and having a thorough understanding of the anatomy and of the different mechanisms of knee injury are essential to the accurate interpretation of knee MR.

REFERENCES

1. Boutin RD, Briggs JE, Williamson MR. Injuries associated with MR imaging: survey of safety records and methods used to screen patients for metallic foreign bodies before imaging. AJR Am J Radiol 1994;162:189-94.
2. Elster AD, Link KM, Carr JJ. Patient screening prior to MR imaging: a practical approach synthesized from protocols at 15 U.S. medical centers. AJR Am J Radiol 1994;162:195-9.
3. Reicher MA, Rauschning W, Gold RH, et al. High-resolution magnetic resonance imaging of the knee joint: normal anatomy. AJR Am J Radiol 1985;145:895-902.
4. Hayes CW, Conway WF. Normal anatomy and magnetic resonance appearance of the knee. Top Magn Reson Imaging 1993;5(4):207-27.
5. Firooznia H. Knee: MRI and CT of the musculoskeletal system. St. Louis: Mosby-Year Book, 1992:661-797.
6. Beyer D, Steinbrich W, Friedmann G, et al. Use of surface coils in magnetic resonance imaging of orbit and knee. Diagn Imaging Clin Med 1986;55:84-91.
7. Mirowitz SA. Fast scanning and fat-suppression MR imaging of musculoskeletal disorders. AJR Am J Radiol 1993;161:1147-57.
8. Heron CW, Calvert PT. Three-dimensional gradient-echo MR imaging of the knee: comparison with arthroscopy in 100 patients. Radiology 1992;183:839-44.
9. Tyrrell RL, Gluckert D, Pathria M, et al. Fast three-dimensional MR imaging of the knee: comparison with arthroscopy. Radiology 1988;166:865-72.
10. Mirowitz SA, Apicella P, Reinus WR, et al. MR imaging of bone marrow lesions; relative conspicuousness on T1-weighted, fat-suppressed T2-weighted, and STIR images. AJR Am J Radiol 1994;162:215-21.

11. Kapelov SR, Teresi LM, Bradley WG, et al. Bone contusions of the knee: increased lesion detection with fast spin-echo MR imaging with spectroscopic fat saturation. Radiology 1993;189:901-4.
12. Morrison WB, Schweitzer ME, Bock GW, et al. Diagnosis of osteomyelitis: utility of fat-suppressed contrast-enhanced MR imaging. Radiology 1993;189:251-7.
13. Hoppenfeld S. Physical examination of the knee: physical examination of the spine and extremities. New York: Appleton-Century-Crofts, 1976:171-96.
14. Netter FH. Musculoskeletal system, Part 1, anatomy, physiology and metabolic disorders: The Ciba collection of medical illustrations. 2nd ed. Summit, Ciba-Geigy Corporation, 1991:94-7.
15. Warwick R, Williams PL, eds. Osteology: Gray's anatomy. 35th ed. Philadelphia: WB Saunders, 1973:357-72.
16. Kaplan PA, Dussault RG. Magnetic resonance imaging of the knee: menisci, ligaments, tendons. Top Magn Reson Imaging 1993;5(4):228-48.
17. Bessette GC. The meniscus. Orthopedics 1992;15(1):35-42.
18. Ellison AE, Berg EE. Embryology, anatomy, and function of the ACL. Orthop Clin North Am 1985;16(1):3-14.
19. Moyer RA, Marchetto PA. Injuries of the posterior cruciate ligament. Clin Sports Med 1993;12(2):307-15.
20. Li KC, Henkelman RM, Poon PY, et al. MR imaging of the normal knee. J Comput Assist Tomogr 1984;8(6):1147-54.
21. Bellon EM, Keith MW, Coleman PE. Magnetic resonance imaging of internal derangements of the knee. Radiographics 1988;8(1):95-118.
22. Zeiss J, Saddemi SR, Ebraheim NA. MR imaging of the quadriceps tendon: normal layered configuration and its importance in cases of tendon rupture. AJR Am J Radiol 1992;159:1031-4.
23. Fitzgerald SW, Remer EM, Friedman H. MR evaluation of the anterior cruciate ligament: value of supplementing sagittal images with coronal and axial images. AJR Am J Radiol 1993;160:1233-7.
24. Hough AJ, Webber RJ. Pathology of the meniscus. Clin Orthop Rel Res 1990;252:32-40.
25. Woods GW, Whelan JM. Discoid meniscus. Clin Sports Med 1990;9(3):695-706.
26. Aichroth PM, Patel DV, Marx CL. Congenital discoid lateral meniscus in children. J Bone Joint Surg [Br] 1991;73B:932-6.
27. Pellacci F, Montanari G, Prosperi P, et al. Lateral discoid meniscus: treatment and results. Arthroscopy 1992;8(4):526-30.
28. Fritschy D, Gonseth D. Discoid lateral meniscus. Int Orthop 1991;15:145-7.
29. Mink JH, Levy T, Crues JV. Tears of the anterior cruciate ligament and menisci of the knee: MR imaging evaluation. Radiology 1988;167:769-74.
30. De Smet AA, Norris MA, Yandow DR. MR diagnosis of meniscal tears of the knee: importance of high signal in the meniscus that extends to the surface. AJR Am J Radiol 1993;161:101-7.
31. Kaplan PA, Nelson NL, Garvin KL. MR of the knee: the significance of high signal in the meniscus that does not clearly extend to the surface. AJR Am J Radiol 1991;156:333-6.
32. Singson RD, Feldman F, Staron R, et al. MR imaging of displaced bucket-handle tear of the medial meniscus. AJR Am J Radiol 1991;156:121-4.
33. Weissman BN, Hussain S. Magnetic resonance imaging of the knee. Rheum Dis Clin North Am 1991;17(3):637-68.
34. Forster BB, Helms CA. Importance of routine T2-weighted or T2*-weighted coronal images in magnetic resonance imaging of the knee. Can Assoc Radiol J 1993;44:396-8.
35. Carpenter WA. Meniscofemoral ligament simulating tear of the lateral meniscus: MR features. J Comput Assist Tomogr 1990;14(6):1033-4.
36. Vahey TN, Bennett HT, Arrington LE, et al. MR imaging of the knee: pseudotear of the lateral meniscus caused by the meniscofemoral ligament. AJR Am J Radiol 1990;154:1237-9.
37. Mesgarzadeh M, Moyer R, Leder DS, et al. MR imaging of the knee: expanded classification and pitfalls to interpretation of meniscal tears. Radiographics 1993; 13:489-500.
38. McGlade CT. Magnetic resonance imaging of the meniscus. Clin Sports Med 1990;9(3):551-9.
39. Lotysch M, Mink J, Crues JV, et al. Magnetic resonance imaging in the detection of meniscal injuries [Oral Abstract]. Magn Reson Imaging 1986;4:185.
40. Helenon O, Bastian D, Laval-Jeantet M. Imagerie par resonance magnetique des menisques du genou. J Radiol 1989;70(4):265-77.
41. Negendank WG, Fernandez-Madrid FR, Heilbrun LK, et al. Magnetic resonance imaging of meniscal degeneration in asymptomatic knees. J Orthop Res 1990;8:311-20.
42. Dillon EH, Pope CF, Jokl P, et al. The clinical significance of stage 2 meniscal abnormalities on magnetic resonance knee images. Magn Reson Imaging 1990;8:411-15.
43. Smith DK, Totty WG. The knee after partial meniscectomy: MR imaging features. Radiology 1990;176:141-4.
44. Bronstein R, Kirk P, Hurley J. The usefulness of MRI in evaluating menisci after meniscus repair. Orthopedics 1992;15(2):149-52.
45. Deutsch AL, Mink JG, Fox JM, et al. Peripheral meniscal tears: MR findings after conservative treatment or arthroscopic repair. Radiology 1990;176:485-8.
46. Farley TE, Howell SM, Love KF, et al. Meniscal tears: MR and arthrographic findings after arthroscopic repair. Radiology 1991;180:517-22.
47. Kent RH, Pope CF, Lynch K, et al. Magnetic resonance imaging of the surgically repaired meniscus: six-month follow-up. Magn Reson Imaging 1991;9:335-41.
48. Applegate GR, Flannigan BD, Tolin BS, et al. MR diagnosis of recurrent tears in the knee: value of intraarticular contrast material. AJR Am J Radiol 1993;161:821-25.
49. Tung GA, Davis LM, Wiggins ME, et al. Tears of the anterior cruciate ligament: primary and secondary signs at MR imaging. Radiology 1993;188:661-7.
50. Lee JK, Yao L, Phelps CT, et al. Anterior cruciate ligament tears: MR imaging compared with arthroscopy and clinical tests. Radiology 1988;166:861-4.
51. Remer EM, Fitzgerald SW, Friedman H, et al. Anterior cruciate ligament injury: MR imaging diagnosis and patterns of injury. Radiographics 1992;12:901-15.
52. Kaplan PA, Walker CW, Kilcoyne RF, et al. Occult frac-

ture patterns of the knee associated with anterior cruciate ligament tears: assessment with MR imaging. Radiology 1992;183:835-8.
53. Boeree NR, Ackroyd CE. Magnetic resonance imaging of anterior cruciate ligament rupture. J Bone Joint Surg [Br] 1992;74-B:614-16.
54. McCauley TR, Moses M, Kier R, et al. MR diagnosis of tears of anterior cruciate ligament of the knee: importance of ancillary findings. AJR Am J Radiol 1994;162:115-19.
55. Chan WP, Peterfy C, Fritz RC, et al. MR diagnosis of complete tears of the anterior cruciate ligament of the knee: importance of anterior subluxation of the tibia. AJR Am J Radiol 1994;162:355-60.
56. Vahey TN, Hunt JE, Shelbourne KD. Anterior translocation of the tibia at MR imaging: a secondary sign of anterior cruciate ligament tear. Radiology 1993;187:817-19.
57. Graf BK, Cook DA, De Smet AA, et al. "Bone bruises" on magnetic resonance imaging evaluation of anterior cruciate ligament injuries. Am J Sports Med 1993;21 (2):220-3.
58. Spindler KP, Schils JP, Bergfeld JA, et al. Prospective study of osseous, articular, and meniscal lesions in recent anterior cruciate ligament tears by magnetic resonance imaging and arthroscopy. Am J Sports Med 1993;21(4):551-7.
59. Shelbourne KD, Nitz PA. The O'Donoghue triad revisited. Combined knee injuries involving anterior cruciate and MCL tears. Am J Sports Med 1991;19(5):474-7.
60. Weber WN, Neumann CH, Barakos JA, et al. Lateral tibial rim (Segond) fractures: MR imaging characteristics. Radiology 1991;180:731-4.
61. Hodler J, Haghighi P, Trudell D, et al. The cruciate ligaments of the knee: correlation between MR appearance and gross and histologic findings in cadaveric specimens. AJR Am J Radiol 1992;159:357-60.
62. Vahey TN, Broome DR, Kayes KJ, et al. Acute and chronic tears of the anterior cruciate ligament: differential features at MR imaging. Radiology 1991;181:251-3.
63. Cheung Y, Magee TH, Rosenberg ZS, et al. MRI of anterior cruciate ligament reconstruction. J Comput Assist Tomogr 1992;16(1):134-7.
64. Autz G, Goodwin C, Singson RD. Magnetic resonance evaluation of anterior cruciate ligament repair using the patellar tendon double bone block technique. Skeletal Radiol 1991;20:585-8.
65. Sanchis-Alfonso V, Martinez-Sanjuan V, Gastaldi-Orquin E. The value of MRI in the evaluation of the ACL deficient knee and in the post-operative evaluation after ACL reconstruction. Eur J Radiol 1993;16:126-30.
66. Howell SM, Berns GS, Farley TE. Unimpinged and impinged anterior cruciate ligament grafts: MR signal intensity measurements. Radiology 1991;179:639-43.
67. Howell SM, Taylor MA. Failure of reconstruction of the anterior cruciate ligament due to impingement by the intercondylar roof. J Bone Joint Surg 1993;75-A(7):1044-55.
68. Gross ML, Grover JS, Bassett LW, et al. Magnetic resonance imaging of the posterior cruciate ligament. Clinical use to improve diagnostic accuracy. Am J Sports Med 1992;20(6):732-7.
69. Grover JS, Bassett LW, Gross ML, et al. Posterior cruciate ligament: MR imaging. Radiology 1990;174:527-30.
70. Sonin AH, Fitzgerald SW, Friedman H, et al. Posterior cruciate ligament injury: MR imaging diagnosis and patterns of injury. Radiology 1994;190:455-58.
71. Burk KL, Mitchell DG, Rifkin MD, et al. Recent advances in magnetic resonance imaging of the knee. Radiol Clin North Am 1990;28(1):379-93.
72. Garvin GJ, Munk PL, Vellet AD. Tears of the medial collateral ligament: magnetic resonance imaging findings and associated injuries. Can Assoc Radiol J 1993;44:199-204.
73. Pavlov H. Sports-related knee injuries. In: Taveras JM, Ferrucci JT, eds. Radiology, diagnosis—imaging—intervention. Philadelphia: JB Lippincott, 1993:1-9.
74. Berlin RC, Levinsohn EM, Chrisman H. The wrinkled patellar tendon: an indication of abnormality in the extensor mechanism of the knee. Skeletal Radiol 1991;20:181-5.
75. Colosimo AJ, Bassett FH. Jumper's knee diagnosis and treatment. Orthop Rev 1990;19(2):139-49.
76. Rosenberg ZS, Kawelblum M, Cheung YY, et al. Osgood-Schlatter lesion: fracture or tendinitis? Scintigraphic, CT, and MR imaging features. Radiology 1992;185:853-8.
77. Shellock FG, Mink JH, Fox JM. Patellofemoral joint: kinematic MR imaging to assess tracking abnormalities. Radiology 1988;168:551-3.
78. Shellock FG, Mink JH, Deutsch AL, et al. Patellar tracking abnormalities: clinical experience with kinematic MR imaging in 130 patients. Radiology 1989;172:799-804.
79. Brossmann J, Muhle C, Bull CC, et al. Evaluation of patellar tracking in patients with suspected patellar malalignment: cine MR imaging vs arthroscopy. AJR Am J Radiol 1994;162:361-7.
80. Delgado-Martins H. A study of the position of the patella using computerised tomography. J Bone Joint Surg 1979;61-B(4):443-4.
81. Conway WF, Hayes CW, Loughran T, et al. Cross-sectional imaging of the patellofemoral joint and surrounding structures. Radiographics 1991;11:195-217.
82. Virolainen H, Visuri T, Kuusela T. Acute dislocation of the patella: MR findings. Radiology 1992;189:243-6.
83. Kirsch MD, Fitzgerald SW, Friedman H, et al. Transient lateral patellar dislocation: diagnosis with MR imaging. AJR Am J Radiol 1993;161:109-13.
84. Lance E, Deutsch AL, Mink JH. Prior lateral patellar dislocation: MR imaging findings. Radiology 1993; 189:905-7.
85. Kaplan PA, Asleson RJ, Klassen LW, et al. Bone marrow patterns in aplastic anemia: observations with 1.5-T MR imaging. Radiology 1987;164:441-4.
86. Munk PL, Vellet AD. Lesions of cartilage and bone around the knee. Top Magn Reson Imaging 1993;5 (4):249-62.
87. Deutsch AL, Mink JH, Rosenfelt FP, et al. Incidental detection of hematopoietic hyperplasia on routine knee MR imaging. AJR Am J Radiol 1989;152:333-6.
88. Shellock FG, Morris E, Deutsch AL, et al. Hematopoietic bone marrow hyperplasia: high prevalence on MR images of the knee in asymptomatic marathon runners. AJR Am J Radiol 1992;158:335-8.
89. Kursunoglu Brahme S, Fox JM, Ferkel RD, et al. Osteonecrosis of the knee after arthroscopic surgery: diagnosis with MR imaging. Radiology 1991;178:851-3.
90. Vellet AD, Marks PH, Fowler PJ, et al. Occult posttrau-

matic osteochondral lesions of the knee: prevalence, classification, and short-term sequelae evaluated with MR imaging. Radiology 1991;178:271-6.
91. Mink JH, Deutsch AL. Occult cartilage and bone injuries of the knee: detection, classification, and assessment with MR imaging. Radiology 1989;170:823-9.
92. Cooper KL. Insufficiency stress fractures. Curr Probl Diagn Radiol 1994;23(2):29-68.
93. Mesgarzadeh M, Sapega AA, Bonakdarpour A, et al. Osteochondritis dissecans: analysis of mechanical stability with radiography, scintigraphy, and MR imaging. Radiology 1987:165:775-80.
94. Hayes CW, Conway WF. Evaluation of articular cartilage: radiographic and cross-sectional imaging techniques. Radiographics 1992;12:409-28.
95. Hodler J, Berthiaume M-J, Schweitzer ME, et al. Knee joint hyaline cartilage defects: a comparative study of MR and anatomic sections. J Comput Assist Tomogr 1992;16:597-603.
96. Hodler J, Resnick D. Chondromalacia patellae. AJR Am J Radiol 1992;158:106-7.
97. Resnick D. Arthrography: bone and joint imaging. Philadelphia: WB Saunders, 1989:154-79.
98. Fielding JR, Franklin PD, Kustan J. Popliteal cysts: a reassessment using magnetic resonance imaging. Skeletal Radiol 1991;20:433-5.
99. Murphy MK, Gross TM, Rosenthal HG. Magnetic resonance imaging of soft tissue and cystic masses about the knee. Top Magn Reson Imaging 1993;5(4):268-82.
100. Burk DL, Dalinka MK, Kanal E, et al. Meniscal and ganglion cysts of the knee: MR evaluation. AJR Am J Radiol 1988;150:331-6.
101. Feldman F, Singson RD, Staron RB. Magnetic resonance imaging of para-articular and ectopic ganglia. Skeletal Radiol 1989;18:353-8.
102. Brown MF, Dandy DJ. Intra-articular ganglia in the knee. Arthroscopy 1990;6(4):322-3.
103. McLaren DB, Buckwalter KA, Vahey TN. The prevalence and significance of cyst-like changes at the cruciate ligament attachments in the knee. Skeletal Radiol 1992;21:365-9.
104. Adam G, Dammer M, Bohndorf K, et al. Rheumatoid arthritis of the knee: value of gadopentetate dimeglumine-enhanced MR imaging. AJR Am J Radiol 1991;156:125-9.
105. Kursunoglu-Brahme S, Riccio T, Weisman MH, et al. Rheumatoid knee: role of gadopentetate-enhanced MR imaging. Radiology 1990;176:831-5.
106. Bjorkengren AG, Geborek P, Rydholm U, et al. MR imaging of the knee in acute rheumatoid arthritis: synovial uptake of gadolinium-DOTA. AJR Am J Radiol 1990;155:329-32.
107. Herve-Somma CMP, Sebag GH, Prieur A-M, et al. Juvenile rheumatoid arthritis of the knee: MR evaluation with Gd-DOTA. Radiology 1992;182:93-8.
108. Poletti SC, Gates HS, Martinez SM, et al. The use of magnetic resonance imaging in the diagnosis of pigmented villonodular synovitis. Orthopedics 1990;13(2):185-90.
109. Jelinek JS, Kransdorf MJ, Utz JA, et al. Imaging of pigmented villonodular synovitis with emphasis on MR imaging. AJR Am J Radiol 1989;152:337-42.
110. Adam PH, Boussaton M, Teisseyre A, et al. Imagerie par resonance magnetique du genou. J Radiol 1991;72(3): 141-7.
111. Resnick D. Bleeding disorders: bone and joint imaging. Philadelphia: WB Saunders, 1989:715-24.
112. Idy-Peretti I, Le Balc'H T, Yvart J, et al. MR imaging of hemophilic arthropathy of the knee: classification and evolution of the subchondral cysts. Magn Reson Imaging 1992;10:67-75.